UNIVERSITY OF THE WITWATERSRAND, JOHANNESBURG

TESTING THE EFFICACY OF THE WORLDVIEW-2 DATA IN DETECTING AND MAPPING THE SPREAD OF *FUSARIUM DIEBACK* IN THE URBAN TREES OF JOHANNESBURG, SOUTH AFRICA

By

ROXANNE-PYAL PARTHAB (1939421)

A research report submitted to the Faculty of Science, University of the Witwatersrand, Johannesburg, in partial fulfilment of the requirements for the degree of Master of Science (Geographical Information Systems and Remote Sensing) at the School of Geography, Archaeology & Environmental Studies.

Supervisor: Prof Elhadi Adam

Co-supervisor: Dr Cletah Shoko

JOHANNESBURG, 2022

TABLE OF CONTENTS

DECLARATION

I, Roxanne-Pyal Parthab, declare that this research report is my own unaided work. It is being submitted for the Degree of Master of Science in Geographical Information Systems and Remote Sensing to the University of the Witwatersrand, Johannesburg. It has not been submitted before for any degree or examination at any other University.

Candidate's Signature: ______________ **Date:** 6/17/2022

ACKNOWLEDGEMENTS

No destination is celebrated without an accomplished journey first. The journey towards completing this MSc research report has been accomplished with great strife and assistance from several people, entities, and organizations. Firstly, to my supervisors Professor Elhadi Adam and Dr. Cletah Shoko, thank you for the continued guidance, feedback and direction towards achieving this goal.

Thank you to the City of Johannesburg Municipality; the Johannesburg City Parks and Zoo; Hilton Fryer of Heuristic Guru (Pty) Ltd and Tree Survey for the free provision of data for this study. In addition, my heartfelt appreciation goes to my colleagues and friends Theo Bernard, Zineth Mpesheni (who has also been such a source of strength and motivation), and John Khorombi for making time to assist with data collection, and for the continuous support throughout this research effort. To my fellow researcher and friend, Gladness Khoza, the depth of knowledge you have shared and put into ensuring that I fully understand the nature of my research is truly appreciated.

To Thirusha Archary (who is my light when all else seems dark, my pillar of strength) and Zaffar Essop – thank you for the constant support and endeavoring assistance whenever and wherever needed from the inception of this study to its completion. Your unwavering encouragement has carried me through this journey.

Theresa Donnelly – without whom I would not have had this opportunity – thank you for seeing my potential all those years ago and taking a chance on me – this journey would not have begun without you. In all that I achieve I am thankful to that first act of kindness.

Lastly, to my parents and sister – Parthab Binah, Sadhana Binah, and Ramona Parthab – thank you for your faith in my studies, your unending support in all my ventures, and the freedom to explore all that I can be, unhindered and unbound. You have been my inspiration through it all. I am because you are.

I thank you all for every valuable input, insight, and idea.

ABSTRACT

Biological invasions, such as plant-pests, are a major threat to urban tree species and can have adverse repercussions on urban ecosystem function, detrimental environmental impacts, and further economic implications in metropolitans if left uncontrolled. Understanding the distribution, abundance, and temporality of these pest-related diseases, such as the *Fusarium Dieback infestation*, are key to assessing the degree of impact on native ecosystems. It is also important that the spread of the disease across large landscapes be tracked and monitored, in order to proliferate and expand management and control efforts. Such undertakings can be achieved using high resolution remotely sensed imagery, such as WorldView-2 (WV-2), and powerful machine learning algorithms such as Random Forest (RF) and Support Vector Machines (SVM), particularly in urbanized areas where there is greater heterogeneity of plant species and therefore higher spectral confusion. This study aimed to test the ability of the eight-band WV-2 multispectral satellite imagery in accurately detecting the occurrences of *Fusarium Dieback infestation* on London Plane (*Platanus* × *acerifolia*) tree species, and subsequently distinguishing these from healthy London Plane (*Platanus* × *acerifolia*) trees, and other tree species. The study focused on London Plane tree species in the Northern suburbs of Johannesburg, South Africa, where presence of the *Fusarium Dieback infestation* is prominent. Additionally, the study also compared the performance of RF and SVM in detecting *Fusarium Dieback* infestation. The study demonstrates the efficacy of using WV-2 in classifying London Plane trees, with an overall accuracy of 87.40% (0.8363 kappa) and 86.61% (0.8259 kappa) for RF and SVM respectively. Infested London Plane trees were mapped with an overall accuracy of 75% for both RF and SVM, showing the potential of WV-2 in distinguishing *Fusarium Dieback* at an intra-species level (i.e. occurring within one species of tree). The results of this study can be used to develop predictive models of early detection and warning for larger urban regions in order to aid management efforts and direct national control mechanisms in curbing the spread of the *Fusarium Dieback infestation*.

Keywords: Remote sensing; Polyphagous Shot Hole Borer; Fusarium Dieback; Random Forest; Support Vector Machine; WorldView-2.

LIST OF FIGURES

LIST OF TABLES

ACRONYM DESCRIPTIONS

WV-2	WorldView-2
RF	Random Forest
SVM	Support Vector Machines
PSHB	Polyphagous Shot Hole Borer
UAV	Unmanned Aerial Vehicle
FABI	Forestry and Agricultural Biotechnology Institute
DALRRD	Department of Agriculture, Land Reform & Rural Development
EPP	Emergency Plant Pest
DEFF	Department of Environment, Forestry & Fisheries
JCPZ	Johannesburg City Parks & Zoo
COI	Cytochrome Oxidase c subunit 1
USA	United States of America
SANBI	South African National Biodiversity Institute
GPS	Global Positioning System
DNA	Deoxyribonucleic Acid
SDM	Species Distribution Models
GIS	Geographic Information Systems
NIR	Near Infra-Red
LULC	Land Use Land Cover
MDA	Mean Decrease Accuracy
VI	Variable Importance
RBF	Radial Basis Function
OOB	Out-Of-Bag
OA	Overall Accuracy
UA	User’s Accuracy
PA	Producer’s Accuracy
ISP	Invasive Pest Species
PSHB	Polyphagous Shot Hole Borer
SWIR	Short Wave Infra-Red

CHAPTER 1:

General introduction

1.1. Background

Urban forests play a vital role in the development and maintenance of sound ecological functions (Gomes et al., 2013). These tree species are responsible for essential services such as filtration of air, temperature reduction and regulation, carbon sequestration, enhanced aesthetic value, and overall improvement of human health (Dale and Frank, 2014). Urban green infrastructure is predominantly made up of street trees that have been historically included in the spatial planning and design of urban regions (Jombo et al., 2020). As a result, urban tree diversity is a heterogeneous mix of both native (indigenous) and non-native (alien) tree species (Jombo et al., 2020). In Johannesburg, the effects of European colonialism has led to an abundance of alien tree species dominating the streets of the affluent northern suburbs (Abutaleb et al., 2020). Many alien tree species still prevail today in the City of Johannesburg because of their ability to spread rapidly and thrive under various climatic conditions (Abutaleb et al., 2020). The spread of these non-native species by historic spatial planning, natural processes, biocontrol efforts, and human activities, have also simultaneously led to the spread of invasive pests that adversely affect urban trees.

Invasive pests have become one of the major threats to urban biodiversity and environmental health (Chance et al., 2016). They reduce urban forest diversity through mortality and subsequent reduced air quality, food security, ecological functioning, and soil productivity (Faithpraise et al., 2013). Urbanization and increased human activities have led to urban forests becoming a prominent pathway for invasive pests, and are therefore critical driving factors for high pest invasions in urban landscapes (Paap et al., 2017). In several South African cities, including Johannesburg, the Polyphagous Shot Hole Borer (PSHB) has rapidly colonized and infested several trees of varying species since it was first discovered (Paap et al., 2018). PSHB is a type of bark beetle known to aggressively invade woody vegetation causing stress, branch dieback, and eventual death of the tree (Paap et al., 2018). This plant pest is native to Vietnam, Asia and was most likely transported to South Africa through the importing of wood, wood products, wooden shipping pallets, trees, and other woody vegetation between the two countries (Paap et al., 2018). The PSHB is responsible for the spread of a disease now known as *Fusarium Dieback*. The PSHB shares a symbiotic relationship with the fungal pathogen *Fusarium Euwallaceae* from which the *Fusarium Dieback* infestation gets its name (Lynch et al., 2016). Almost all tree species that showed the presence of the PSHB also showed the presence of the *Fusarium* sp. in underlying tissue (Eskalen et al., 2013).

Research has indicated that *Fusarium Dieback* affects several species of trees, and can be seen colonizing and infesting street trees in Johannesburg (Fryer, 2019). Visible symptoms of the disease include holes bored into the trunk and branches of the tree with a white powdery deposition around the holes; wilting and discoloured leaves; oozing resin; branch dieback; watery sap staining the tree bark; beetle tunnels under tree bark; and the presence of the beetle sometimes on the surface of the wood (Eskalen et al, 2013; Paap et al., 2018; Fryer, 2019; Paap et al, 2020). Of the many tree species affected by *Fusarium Dieback* in Johannesburg, most damage was recorded on Box Elder (*Acer Negundo*), London Plane (*Platanus x acerifolia*), Chinese Maple (*Acer buergerianum*); and English Oak (*Quercus robur*) (Fryer, 2019). One likely reason for attack on these particular tree species is the abundance in which they appear along Johannesburg streets and open spaces making these susceptible and easy targets (Fryer, 2019). In addition to this, these tree species – among several others – have been listed as reproductive host species thereby making them more favourable to the pest than other trees (Fryer, 2019). A reproductive host tree refers to those tree species in which the PSHB can successfully reproduce, and which eventually die from *Fusarium Dieback* (Paap et al., 2018). Non-reproductive host trees are those tree species which are attacked by PSHB, but in which the beetle does not reproduce – the tree suffers the effects caused by the *Fusarium Euwallaceae* fungus, but is not likely to develop *Fusarium Dieback infestation*, and has the potential to recover (Fryer, 2019).

The ability to accurately identify and map individual trees at a species level is pivotal to the development of viable urban forest management strategies, as well as biodiversity monitoring and pest control (Shi, 2020). Mapping the distribution of the PSHB invasion across street trees is a critical factor in minimizing the spread of the *Fusarium Dieback infestation* in complex urban environments such as the Johannesburg city. Additionally, it will aid in urban spatial development and sustainability planning within the city, as well as effective resource allocation (Li et al., 2015; Abutaleb et al., 2020). Thus, there is a growing need for updated urban tree inventories that recognize the species and health (i.e. the presence of pest invasion or not) of individual trees in order to understand the broader effects of this pest invasion in various urban tree species. Vegetation mapping of complex and compound urban environments forms an integral part of accurate and efficient urban planning.

Different approaches exist for the detection and mapping of tree species and associated pest invasions. These approaches include traditional field-based identification of healthy and infested trees; visually interpreting aerial imagery; flying unmanned aerial vehicles (UAVs); using hyperspectral satellite imagery; and most recently, the use of multispectral satellites and sensors in conjunction with various machine learning classification algorithms (Myeong et al., 2006; Alonzo et al., 2014; Chance et al., 2016; Jombo et al., 2020). The conventionally used ground-based approaches are time-consuming particularly because it requires on-site investigation of individual trees, and costly because it usually requires specialized knowledge, trained professionals, and expensive equipment (Hartling, 2019). It is also prone to human-related errors, and is not as spatially accurate as newer technological approaches (Alonzo et al., 2014). Furthermore, research is limited to physically accessible areas and are inadequate in mapping pest occurrences where there are urban forests in remote locations (Hartling, 2019). Conventional approaches have been replaced and/or combined over time with advancements in remote sensing technology that provides spatially-continuous data collection, and is able to provide remote access (Shi, 2020).

Remote sensing approaches have become a globally recognized and extensively used mechanism for large-scale mapping (Chance et al., 2016). The visual interpretation of aerial imagery was widely used in the 1990's as an early form of remote sensing for mapping of urban forests (Shi, 2020). However, visual interpretation was not without criticism for factors such as being time-consuming, and highly subjective (Shi, 2020). Furthermore, visual interpretation is unable to reveal full information about individual tree characteristics; or overcome variability of trees of the same species; as well the similarities of different tree species (Shi, 2020). While UAVs and hyperspectral data are both more advanced approaches, they are also limited by computer processing costs, time, data dimensionality, and spatial coverage extent (Alonzo et al., 2014; Jombo et al., 2020; Abutaleb et al., 2020).

Multispectral satellite imagery, on the other hand, provides timely, finer and more accurate data, with global daily coverage (Hartling, 2019). It also provides higher spectral resolution and the capability of assessing individual objects per pixel for precise analysis of tree species and forest mapping (Chance et al., 2016; Jombo et al., 2020). Multispectral sensors therefore provide a more economical solution to the collecting of individual tree information by capturing spectral and structural signatures of individual trees (Shi, 2020). Remote sensing systems, such as the WorldView-2 multispectral product, are a necessary opportunity for developing countries like South Africa to invest in high data-quality technology and synthesizing tools that provide higher-accuracy data mapping, predictive modelling, and priority zone delineation in the effective management of invasive plant species (e.g. mapping *Fusarium Dieback* infestation distribution across different tree species) (Anderson and Gaston, 2013). Several studies have shown that WorldView-2 is highly accurate when combined with the right classifier to delineate and map various trees species, plant-pest invasions, and other vegetation studies with a greater than 80% accuracy outcome (Boggs, 2010; Abutaleb et al., 2020; Jombo et al., 2020). Some such examples of successful tree species detection with remote sensing include the mapping of Bracken Fern using WV-2 and Random Forest with an 84.72% accuracy (Odindi et al., 2014); identifying the distribution of eucalyptus trees with WV-2 at an 81.67% success rate with Random Forest, and 80% accuracy with Support Vector Machines algorithm (Abutaleb et al., 2020); and the mapping of various tree species in heterogeneous urban environments with WV-2 at an 84.2% accuracy using Random Forest algorithm, and 81.2% accuracy with Support Vector Machines (Jombo et al., 2020). As such, this study focused on testing the ability of the WV-2 multispectral imagery in mapping and distinguishing between healthy London Plane trees and those infested by the *Fusarium Dieback* pest disease, in Johannesburg, South Africa.

1.2. Research Problem statement

The Polyphagous Shot Hole Borer (PSHB) invasion has been a threat to Johannesburg's green infrastructure since 2017 when it was first detected (Paap et al., 2018). A sentinel tree planting programme for the recording of pest-host interactions in botanic gardens led to the discovery of damage to London Plane (*Platanus x acerifolia*) trees (Paap et al., 2018). Since then the PSHB pest has spread to all South African provinces, except Limpopo (Paap et al., 2018). A list of reproductive and non-reproductive host trees (last updated in April 2019) have been created and verified by the Forestry and Agricultural Biotechnology Institute (FABI), which include some 21 indigenous and exotic tree species across the country (Fryer, 2019). According to recent studies, more than 100 tree species have been attacked by the PSHB in South Africa, with the greatest impact of the pest invasion affecting urban environments such as Johannesburg, George, and Knysna where the biggest outbreaks were recorded (Paap et al., 2020). Since the pest was first detected four years ago, research has suggested that the *Fusarium Dieback infestation* has become one of the most damaging tree invasions in South Africa, causing widespread and uncontrolled tree mortality (Paap et al., 2020).

Due to the rapid rate at which the tree-pest has spread throughout the country, little coordinated response or strategic management plans have been made yet (Paap et al., 2020). The complication of understanding which government agency is responsible for monitoring and management of urban forests, as well as the lack of formal response from various stakeholders (such as Department of Agriculture, Land Reform and Rural Development (DALRRD), The South African Emergency Plant Pest (EPP) Response Plan, Department of Environment, Forestry, and Fisheries (DEFF), local authorities, and industry professionals) has led to minimal efforts in the creation of monitoring, control and eradication plans (Paap et al., 2020).

Already in several parts of Johannesburg there has been widespread tree mortality with the removal of more than 1000 infested/dead trees across the city due to the outbreak of the PSHB and its consequent *Fusarium Dieback infestation* (Fryer, 2019). Research has indicated that possibly more than half a million trees in Johannesburg are already infested and the numbers are expected to rise (Fryer, 2019). While no concerted effort at mapping the actual numbers of infested trees have been done yet, it is visible in the Johannesburg urban landscape that tree mortality rates has been high (Fryer, 2019). Northern Johannesburg suburbs (such as Parkwood, Sandton, and Greenside) have distinct gaps in otherwise clustered rows of street trees where the trees have been removed in an attempt to prevent the spread of the disease (Paap et al., 2020).

Currently, spatial knowledge about *Fusarium Dieback* in Johannesburg exists, but is limited due to the limiting nature of traditional data collection methods (Fryer, 2019). Traditional methods often include on-site surveys that require the physical presence of data collectors across huge study areas; specialized knowledge and training on various data collection techniques; and specific data collection devices/software. Considering the size of Johannesburg, and the extensive number of tree species that exist within it, such conventional field survey methods will not be sufficient to adequately and accurately map the spatial trends of the disease. There is also currently little evidence of studies being done to investigate the applicability of remote sensing methods, and use of high spatial resolution technology, to detect and possibly predict the spread of the *Fusarium Dieback* infestation in South Africa. FABI initiated several baseline studies since 2017 but most are restricted to surveillance and monitoring, while current projects are focused on finding biological control agents of the PSHB (Paap et al., 2020). Thus, there is the need to investigate remote sensing as an extensive, timely and low-cost alternative for the mapping and monitoring of the infestation.

1.3. Aim and Objectives:

The specific objectives were guided by the following research questions:

- How accurately can WV-2 distinguish between London Plane trees and other LULC classes?
- Which classification algorithm, RF or SVM, performs better when combined with WV-2?
- Can WV-2 be used to detect *Fusarium Dieback* by accurately differentiating between healthy and infested London Plane trees?

The overall aim of the study was to determine how accurately WorldView-2 satellite imagery can be used to detect the *Fusarium Dieback* infestation in the London Plane (*Platanus x acerifolia*) tree species in the Northern suburbs of Johannesburg.

The objectives of the study are to:

- Assess the ability of WorldView-2 (WV-2) satellite imagery in differentiating between London Plane trees and other LULC in the Northern suburbs of Johannesburg using both Random Forest and Support Vector Machine classifiers.
- Test the accuracy of WorldView-2 satellite imagery in detecting the *Fusarium Dieback* infestation by differentiating between healthy and infested London Plane trees using both Random Forest (RF) and Support Vector Machines (SVM) classifiers.
- To determine which machine learning algorithm, RF or SVM, performs better when combined with WV-2 imagery.

1.4. Research Report Structure

This research report is made up of 7 chapters.

Chapter 1 is the introductory chapter which includes the introduction to the research, and details the background, rationale, problem statement and the outlines of the report, as well as the main research questions, aim and objectives.

Chapter 2 is the Literature Review which synthesizes existing information about the PSHB, *Fusarium Dieback infestation*, and WV-2 solutions, providing deeper understanding of the research.

The Methodology forms Chapter 3, covering details about the study site, the data acquisition processes, and the methods used to undertake the overall research in order to reach specific research objectives.

Chapter 4: Results, outlines and explains the findings of the research derived through the results of the research methods undertaken.

Chapter 5 is the Discussion Chapter which comprises a detailed discussion on what the findings are and how the findings and results of the research meet the desired outcome of the main aim, objectives, research expectations, etc.

Chapter 6 is the Conclusion which provides recommendations and gives an overall conclusion to the main outcomes of the research project, determining if the research met the initial goals set out.

CHAPTER 2:

Literature Review

2.1. The ecology of the Polyphagous Shot Hole Borer and its impacts

Cities are found to be hotter than rural areas making it more habitable for plant pests that thrive in warm temperatures, thus allowing increasing pest fecundity (Dale and Frank, 2014). While some plant pests are easier to control or eradicate, other species of pests are known to be aggressive invaders, colonizing large populations of trees and establishing hosts in more than one tree species (Eskalen et al., 2013). Some examples include the *Homoptera: Aphididae* or Greenbug (Yung et al., 2005); *Trialeurode Vaporariorum* or White Fly (Boissard et al., 2008); *Sirex noctilio* or Woodwasp (Dye et al., 2008); *Coryphodema tristis* or Cossid Moth (Boreham, 2006; Adam et al., 2013); *Melanaspis tenebricosa* or Gloomy Scale (Dale and Frank, 2014); *Polyphagous Shot Hole Borer (*PSHB*)* (Eskalen et al., 2013); among a plethora of other known species that actively reduce the tree genera in urban landscapes.

The *Polyphagous Shot Hole Borer (*PSHB*)* is an ambrosia beetle from the *Coleoptera: Scolytinae* family, more commonly known as 'Bark Beetle' (Eskalen et al., 2013). According to Raffa et al. (2015), Bark Beetles originate from a diverse subfamily of weevils that spend their entire life cycle within plants. Chen et al. (2020) note that new taxonomic classifications for the Shot Hole Borer family (Polyphagous, Tea, and Kuroshio) were proposed in 2015 (O'Donnell et al., 2015), 2017 (Stouthamer et al., 2017) and again in 2019 (Smith et al., 2019) due to the morphological similarities that they share. Studies into the ecology and make-up of the Shot Hole Borer family show differences in the cytochrome oxidase c subunit 1 (COI), and in their cuticular hydrocarbon profiles (Chen et al., 2020). Studies have yet to determine which of the borers are most aggressive and to what varying degrees (Chen et al., 2020).

While these beetles exist in almost all regions of the world, they most commonly occur in terrestrial plants such as trees, and are associated with microbial symbionts (Raffa et al., 2015). PSHB carries with it a fungal symbiont known as *Fusarium Euwallaceae* which is responsible for causing a plant disease known as *Fusarium Dieback* (Eskalen et al., 2013). *Fusarium Dieback* occurs when the beetle attacks a tree's vascular system, preventing it from absorbing nutrients and water, consequently leading to stress, dieback, and eventual death of the tree (Paap et al., 2018).

2.2. Symptoms and spread of the *Fusarium Dieback* infestation

The PSHB beetle was first reported in California, USA on Black Locust (*Robinia Pseudoacacia*) trees in 2003, but identification of fungal damage only occurred in 2012 on avocado trees exhibiting symptoms of branch and leaf dieback (Eskalen et al., 2013). It has since spread or been introduced secondarily to several other USA counties including Orange, Riverside, San Bernardino, San Diego, and Ventura counties (Chen et al., 2020). PSHB is native to East Asia but was unintentionally introduced to several countries around the world, including the USA, Israel, and South Africa (Paap et al., 2018). It is believed that the earliest transmittance of the pest-disease complex between continents was through the import and export of timber and other woody products (Umeda, 2017; Paap et al, 2018). Attacks by the PSHB was only identified in South Africa in 2017 in the botanical gardens of Pietermaritzburg, KwaZulu-Natal through a sentinel project initiated by the South African National Biodiversity Institute (SANBI), and later in suburbs within the City of Johannesburg, Gauteng (Paap et al., 2018; Paap et al., 2020). Because the invasive PSHB are resilient to climatic factors, they are able to thrive in several different climates outside its native country (Paap et al., 2018). According to Raffa et al. (2015) variations of the general beetle life cycle exists but most species of beetle, including the PSHB, only appear from their brood galleries during spring/summer periods to seek new mating partners as well as new host trees. A study conducted in California, USA by Lynch et al. (2018), indicated that occurrences of the *Fusarium Dieback* infestation and the presence of the PSHB were neither temperature- nor humidity-dependent, and was also inconsistent with tree density, species, and size. The study revealed that the spread of the disease was spurred instead by host availability – that is, the availability of trees that could serve as hosts for the pest and its associated fungi (Lynch et al., 2018). While the study aimed at identifying different environmental factors influencing the distribution of PSHB across different geographic spaces, it can be criticized for its lack of focus on spatial characteristics, spectral variances in the tree species acting as reproductive hosts, and does not answer broader locality concerns of where the most vulnerable forests are / will be found. Additionally, the study has not been replicated outside of California to determine if the parameters apply to climates and landscapes globally. In contrast, other studies have shown that the PSHB breeds optimally between 13° C and 33° C, with its optimal development temperature being 28° C, suggesting that the pest is able to thrive in hot regions and spread during warmer months (Umeda, 2017).

The life cycle of the beetle begins with the beetle boring small holes, known as entry holes, into the bark of the host tree. It continues boring deeper through the cambium, and ultimately entering the xylem

(Eskalen et al., 2013). As it bores its way through the tree, it creates tracts in the bark of the host tree where the female borer establishes a breeding and feeding gallery (Eskalen et al., 2013). Once inside the xylem, the PSHB releases the *Fusarium Euwallaceae* into the vascular system where the fungus then attacks its host by entering the underlying tissue, producing mycelia, and preventing healthy functioning of the trees system (Paap et al., 2021). Chen et al. (2020) indicated that the high rate of tree mortality associated with *Fusarium Dieback* is largely caused by this disruption and/or prevention of water and nutrients in the trees' xylem and phloem. The fungus also serves as a source of food to the beetle and its larvae. According to Umeda (2017) the *Fusarium Euwallaceae* fungus is able to provide the adequate nutrition level required for development of its larvae to adulthood in host tree species, thus enabling and exacerbating the spread of *Fusarium Dieback* (Umeda, 2017). Paap et al. (2021) has noted that PSHB only completes its life cycle in reproductive host trees. The female PSHB acts as a vector and continues the spread of the fungus throughout the tree and to other trees (Eskalen et al., 2013). Wichmann and Ravn (2001) noted that the dispersal of the female vector across a few hundred meters from its initial host tree is where the most intense and successful attacks occur, but the potential of the beetle to fly several kilometers does exist (Wichmann and Ravn, 2001).

Symptoms of the invasion are characterized by visible staining and discoloration, gum deposition, and white powder know as sugar volcanoes around entry holes, as well as browning of underlying tissue (Eskalen et al., 2013), as shown in Figure 1. Additionally, signs of dieback include early wilting, drying, and shedding of leaves; complete loss of leaves; oozing resin from trunk and branches; and fungal streaks in sapwood (Paap et al., 2021), as evidenced in Figure 2. The PSHB colonizes trees that are most likely already under stress from pre-existing biotic and/or abiotic factors (Raffa et al., 2015). According to Mendel et al. (2012), avocado plantations in Israel showed signs of dieback in 2005, accompanied by the accumulation of white powder around bored holes in the barks of several trees (Mendel et al., 2012). The beetle's aggressive invasion and ability to attack different species of trees in California (Eskalen et al., 2013), Israel (Mendel et al. 2012) and South Africa (Paap et al., 2018), suggest that the likelihood of establishing itself in both local and global tree populations exist. This exacerbates the growing threat that the pest-fungus complex poses to green infrastructure in South African urban environments (Matthews et al., 2015).

Figure 1: Visible symptoms of *Fusarium Dieback* on the bark and branches of infested trees

Figure 2: Visible symptoms of *Fusarium Dieback* on the leaves of infested trees

FABI, TreeSurvey, and JCPZ identified various stages of infestation that a tree can be experiencing. This was diagnosed and based on the severity of the symptoms that the tree presented (Fryer, 2019). While each institution created their own description, they used a similar classification system for the stages (Fryer, 2019). Stages 1 and 2 indicated the presence of the infestation with presentation of some symptoms, but a greater than 50% chance of survival; with levels 3 and/or 4 indicating extreme dieback with minimal chance of survival, or death of the tree (Fryer, 2019).

In South Africa, the disease has had a widespread impact on the public tree populations within the various provinces. Gauteng, with Johannesburg's dense urban forest in particular, has been affected the most severely (Paap et al., 2020). By July 2019, Tree Survey had recorded at least 100 different tree species in the country that were infected with *Fusarium Dieback infestation*. Of these, Tree Survey listed 21 known reproductive host species (Fig. 3). Of the reproductive host species, the most affected are the *Acer*

Negundo (Box Elder), followed by the *Acer buergerianum* (Chinese Maple), *Quercus robur* (English Oak), *Albizia adianthifolia* (Flat Crown), and the *Platanus x acerifolia* (London Plane) (Fryer, 2019).

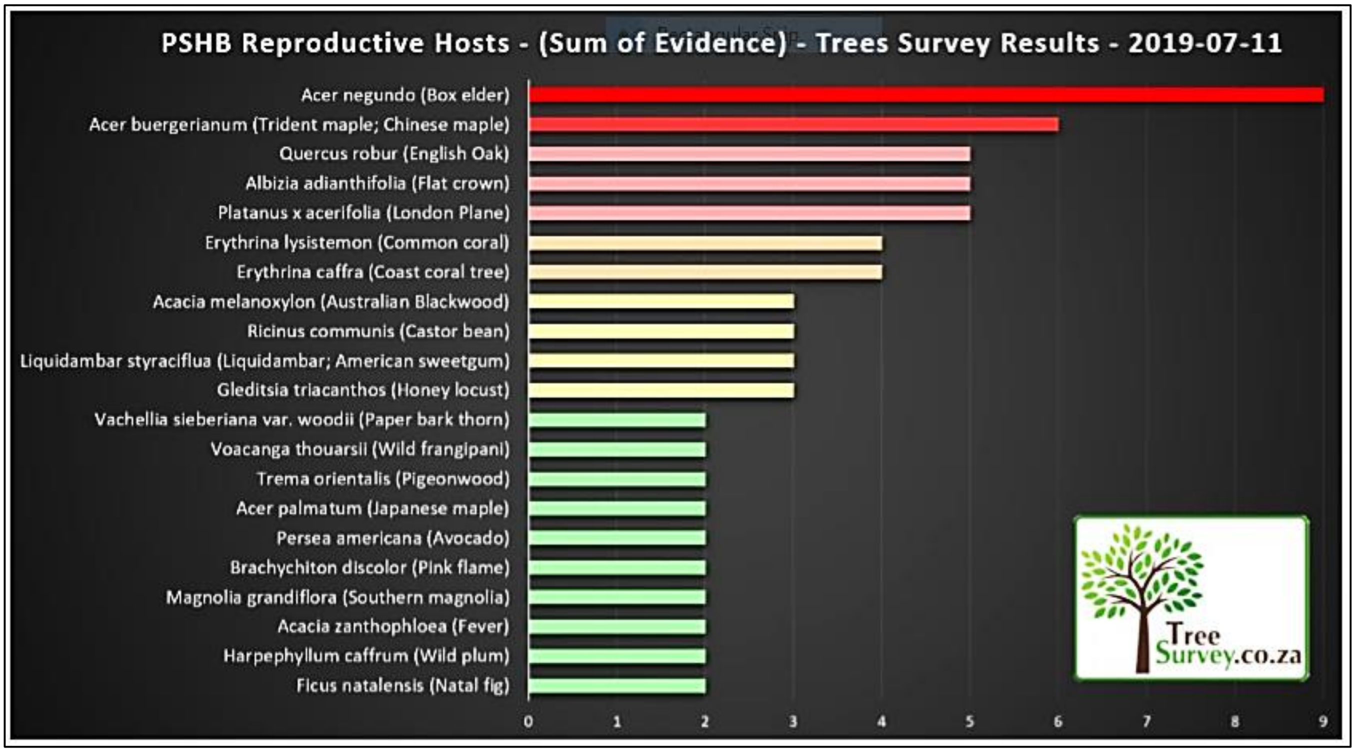

Figure 3: List of reproductive host trees identified in South Africa by 2019 (Fryer, 2019)

2.3. The London Plane tree species – a reproductive host

The *Platanus x Acerifolia*, more commonly known as London Plane, is a tree species of the *Platanus* genus and is used globally as a landscape tree because of its adaptability to various climates and resilience to urban conditions (Tsopelas et al., 2017). It is found predominantly along urban streets, in city parks, and botanical gardens, and has been widely used for the removal of small pollution particles in urban regions, thus making it a popular and common part of city green infrastructure (Tsopelas et al., 2017). The London Plane is a hybrid of *Platanus orientalis* (oriental sycamore) and *Platanus occidentalis* (American sycamore) believed to have first been cultivated in Spain and London and is the most popular *Platanus* tree globally (Tsopelas et al., 2017). This species of tree are large deciduous trees, growing to more than 40m in height, with a trunk circumference of 3m or more (Carinanos et al., 2020). It can be distinguished from other trees of the same family by the grey-green colouring of its bark, and the stiff-textured, often thick, lobed-shaped leaves (Carinanos et al., 2020).

In Johannesburg, many older suburbs are lined with London Plane trees, particularly in the affluent northern parts of the city (Schäffler and Swilling, 2012). The introduction of London Plane trees in South Africa is a result of historic spatial planning and colonial rule (Schäffler and Swilling, 2012). London Plane trees are known to be resilient to several common plant diseases and tend to grow and spread quickly in urban soils, therefore being a popular choice for urban street plantation (Schäffler and Swilling, 2012). In addition to this, London Planes are easily transplanted and withstand several types of soil conditions, thus aiding the successful and proliferated movement of the tree species from London to South African cities (Schäffler and Swilling, 2012). The species has been able to thrive in Johannesburg successfully for decades until recent reports indicate the death of many London Plane trees in botanic gardens and urban streets due to the *Fusarium Dieback infestation* (Paap et al., 2020). Because more than 16% of Johannesburg's landscape is covered by trees, the high mortality rate has affected several ecosystem functions, particularly the regulation of water flow and surface run-off in residential areas characterized by hard surfaces (i.e. buildings, roads, tarred surfaces) (Schäffler and Swilling, 2012).

2.4. Environmental and economic impacts of the *Fusarium Dieback* infestation

Recent research has indicated that the environmental implications of the PSHB invasion are serious, detrimental, and pose a large-scale threat to urban tree species, and agricultural plantations, worldwide (Umeda, 2017; Paap et al., 2020; Lynch et al., 2021). In addition to this, the invasive beetle has the potential to destroy green infrastructure in several urban regions, as well as widespread ecosystem malfunction that will have secondary or ripple-effect outcomes (Umeda, 2017). Because the beetle is relatively indiscriminant in the types of woody vegetation it colonizes and infests, the possibility of *Fusarium Dieback* attacking commercial plantations is high, with great risk to the disruption in food supply; the export of certain fruits, vegetables, etc.; and the timber industry (Umeda, 2017). The possible loss of entire native tree species is also an existing threat of the PSHB invasion. This comes with associated challenges including the loss of vital ecosystem functions, permanent alteration to ecosystem and forest landscapes, biodiversity loss, destruction of natural habitats, reduced open spaces in urban regions, potential spread of human- and plant-related diseases, urban forest loss and gap formation, and increased competition for limited resources, amongst a plethora of other adverse effects (De Wit et al., 2021).

A further concern that researchers in South Africa have expressed is the lack of data and economic assessments that exist (De Wit et al., 2021). Understanding the economic aspects of the PSHB invasion aids in determining how economic activities drive the spread of plant-pest invasions, as well as in calculating the magnitude of the costs incurred by PSHB-related ecological damage (De Wit et al., 2021). Research postulates that existing economic models are biased towards *ex post* assessments and thus fail to account for the forecasted or possible economic detriments of the PSHB (De Wit et al., 2021). Because of the failure to account specific government agencies with responsibility into the studies of PSHB, economic modelling has not been given the necessary priority – a consequent of which is the likely loss of vast amounts of money that will be required for the removal of dead trees, replantation efforts, and post-damage rehabilitation including social, environmental, and economic efforts (De Wit et al., 2021).

The economic forecast model developed by De Wit et al. (2021) suggest that a potential cost of 27.12bn dollars, or 1% of South Africa's Gross Domestic Product (GDP), will be required for the removal of urban trees that die from *Fusarium Dieback*. This not only presents a huge economic loss across the country, but also illustrates the massive threat to urban trees that PSHB poses over the next few years. *Fusarium Dieback* has been recognized as the largest global pest outbreak, currently, and is especially invasive in urban forests (De Wit et al., 2021).

The environmental threat facing Johannesburg as a result of the PSHB outbreak is particularly serious because of the limited information available on invasion dynamics within urban areas, as well as the ecological dependencies that exist (Gaertner et al., 2017). In addition to this, trees showing *Fusarium Dieback infestation* usually need to be removed to curb the spread – this means that fewer street trees exist to maintain ecological controls such as the reduction of flash flooding, regulation of drainage, increased contamination of ground water, resilience to erosion, management of air-filtration, and regulation of the city's microclimates (Schäffler and Swilling, 2012). Paap et al. (2020) noted the potential for extreme alterations in urban ecosystems and the breakdown of vital ecological co-dependencies between trees of different species, as well as the different environmental components that sustain the city (Paap et al., 2020).

2.5. Detection and monitoring approaches for *Fusarium Dieback* infestation

Current methods of detecting *Fusarium Dieback* in trees include physical assessment of trees on the ground (Eskalen et al., 2013). This requires a person to visually identify the beetle, or symptoms of stress and dieback on each tree. The principal approach in detecting pest-diseases undertaken at a local scale is field-based in which observations are made with the naked eye or require physically monitoring symptoms on the ground by trained professionals (Faithpraise et al., 2013). Other field-based approaches include field-survey techniques wherein observers are able to collect location data of infected trees and plants.

However, such methods are not always geographically accurate due to the high probability of errors by non-specialized observers (Faithpraise et al., 2013). Not only are these methods time-consuming and vulnerable to inaccuracies, but can also become expensive and labour-intensive (Faithpraise et al., 2013). Non-conventional methods of pest-disease detection are becoming more widely-used and have greater potential for accuracy and scope, including the use of remotely sensed data, aerial and satellite imagery, as well as other high-resolution remote sensing tools (Atkinson et al., 2017).

FABI have identified and described several symptoms and signs of infection that can be used to determine if a tree has been infected or not (Fryer, 2019). This is then reported to TreeSurvey using the mobile application that records the GPS location of the tree, or a sample of the tree bark is sent to FABI laboratories where DNA sequencing is undertaken to determine the presence of the PSHB (Fryer, 2019; Eskalen et al., 2013). According to FABI, the PSHB invasion is a relatively new incident in South Africa, and therefore limited monitoring approaches exist (FABI, 2019). The largest known global cases occurring in California (Eskalen et al., 2013; Boland, 2016) and Israel (Mendel et al., 2012; Freeman et al. 2012) include the monitoring of agricultural avocado plantations that were severely affected in these areas. While these approaches have been largely successful, they do not effectively suit the South African situation where it is the urban forests that are impacted the most (Paap et al., 2020). Thus, there is a lack of effective monitoring measures in place to contain the spread of the beetle and the subsequent disease.

2.6. Approaches to the control and management of PSHB infested tree species

Boland (2016) points out the need for early detection and rapid response programmes, as well as pre-emptive rehabilitation strategies to regrow severely reduced urban forests (Boland, 2016). Byers et al. (2018) take the discussion on control and management approaches further with suggestions of push-pull methods that prevent PSHB mating from occurring which could serve as a more permanent mitigation measure (Byers, 2018). Foxcroft et al. (2017) postulated that one of the major concerns with aggressive invasions is not only that it happens sporadically and speedily, but also the difficulty in detecting the ecological and functional changes that the invasion causes. Consequently, invasive species are only detected at an advanced stage of the invasion during which time mitigations measures are either too late or too ineffective.

Biological control is also an important management strategy that could be crucial in minimizing PSHB populations, particularly when pesticides and chemical solutions are dangerous to the tree populations involved (Foxcroft et al., 2017). There are currently no known chemical solutions that have been approved to kill the beetle-fungus complex, nor has there been any identification of biological predators of the beetle in South Africa (Paap et al., 2020). Paap et al. (2020) point out that chemical trials have only just begun in South Africa with most knowledge on its effects being taken from Californian studies. It has been noted here that chemical control is only effective as a preventative measure or at the earliest stages of infestation largely because the PSHB spends little time on the surface of trees where pesticides would be most prominent (Paap et al., 2020). Furthermore, borers do not ingest vast amounts of wood as they feed on the fungi that they self-produce, thus chemical treatments have proven to have little effect on PSHB despite posing great threats to the tree itself (Paap et al., 2020).

According to Lynch et al. (2018), another method of management is to get rid of tree branches carrying the PSHB. As such, the entire tree does not need to be removed (given that the trunk and vascular system of the tree is still healthy) but only the branches on which the beetle lives, thus reducing the possibility of further colonization of the tree, as well as aiding in the reduction of the PSHB population (Lynch et al., 2018). The application of pruning, in conjunction with spray treatments, has been widely applied to avocado plantations in America, with relative success, and is recommended by researchers as a viable solution to branch dieback (Lynch et al., 2018). Lynch et al. (2018) illustrated pruning of infested branches, followed by immediate spray treatment, resulted in a significant reduction in beetle attacks, as well as an increased number of abandoned borer entryways into a tree's gallery after pruning and spraying.

Chen et al. (2020) investigated the possibility of using chipping or grinding methods to curb the spread of *Fusarium Dieback infestation*. Chipping is a process by which trees are cut into small cubes of wood, or broken down into manageable pieces, in order to reduce the movement of infested wood/trees across areas of high infestation potential (Chen et al., 2020). While these methods do not stop the spread or eradicate infestation, it can considerably slow down the rate of spread and subsequent infestation of surrounding trees (Chen et al., 2020). Their research showed that the effects of grinding infested wood down to 7.6cm or smaller pieces significantly reduced the emergence of the beetle. Chipping to 5cm and smaller disrupted the PSHB activity (Chen et al., 2020). The success of the chipping method in South Africa, and on London Plane tree species, is unknown.

Existing control measures are not sustainable or long-term solutions because they include the permanent removal, and subsequent burning, of infected trees. However, they remain the most crucial current practice because it has been the most effective control mechanism thus far, despite the threat of ecological damage that persists (Paap et al., 2020). This practice has resulted in a fast-diminishing urban forest without the possibility of natural regrowth or replacement over time. Such methods also pose a threat to native tree species and the reduction in indigenous biodiversity (Paap et al., 2020). Local municipalities and control agencies have begun investing in tree removal projects, as well as the possibility of tree replacement projects to combat the effects of the *Fusarium Dieback* infestation in Johannesburg and other parts of South Africa (Paap et al., 2020). Collaborative efforts between government agencies, municipal sectors, and other research institutes have led to the implementation of several ongoing research projects aimed at impact assessment, as well as developing effective determination, monitoring, and management measures that can be applied across the South African landscape (Van den Berg et al., 2018; Paap et al., 2020).

2.7. Remote Sensing techniques for detecting pest-diseases in urban tree species

A leading alternative to the field-based approach is the use of high resolution satellite imagery that has the capacity to detect pests in large urban forests. Remote sensing technology has emerged as a leading alternative to tradition methods because of its cost-effective approach to the collection of spatial data (Hartling, 2019). Furthermore, remote sensing is efficient, repeatable, and rapid in the monitoring and detection of urban tree dynamics, particularly in dense urban forests with several tree species clustered together (Myeong et al., 2006). Satellite mapping capabilities provide predictive tools that aid the assessment of pest invasion dynamics in order to enhance species invasion management (Monteiro et al., 2017). Remote sensing offers a wide-area monitoring of environmental changes for tree species mapping, and forest health analysis (Monteiro et al., 2017).

There are numerous satellite sensors available with different spectral and spatial resolutions. These include medium/coarse resolution imagery such as LANDSAT TM (30m) or MODIS (250m), as well as high resolution imagery such as WorldView-2 (2m) (Monteiro et al., 2017). The multispectral capabilities provided by high resolution sensors has popularized the WorldView-2 satellite imagery in recent years. This is attributed to its eight spectral bands, including the new red edge band, which are configured with the unique part of the electromagnetic spectrum. The red edge band has become extensively used in measuring plant health and mapping urban vegetation (Abutaleb et al., 2020). Furthermore, the red-edge band is known to better discriminate between healthy and diseased trees than courser resolution sensors (DigitalGlobe, 2010). WorldView-2 not only overcomes the limitations of courser resolution sensors, it also does not experience the same challenges of hyperspectral sensors, such as misclassification errors and dimensionality issues, (Mutanga et al., 2012).

WorldView-2 satellites acquire data at a high spatial resolution across 8 different bands, including the red edge band (DigitalGlobe, 2010). This enables the sensor to detect fine details about vegetation physiological characteristics as well as the identification of individual trees species. The high spectral resolution is also ideal for the determination of tree health in various species and areas.

Extensive research has been done over the years to improve approaches to the detection, monitoring, and subsequent mapping of urban tree species (Immitzer et al., 2012; Liu et al., 2015; Adam et al., 2017; Abutaleb et al., 2020; Jombo et al., 2020; etc.). Several researchers have used WorldView-2 (WV-2) satellite imagery with a classification algorithm such as Random Forest (RF) in order to produce classifications with high levels of accuracy. Mutanga et al. (2012) used the WV-2 red edge band, with the Random Forest classifier, to estimate biomass in vegetated wetlands. The outcome showed a greater than 80% accuracy and proved the applicability of WV-2 in mapping biomass at a high density, which broad band satellites are not able to do (Mutanga et al., 2012). Lofgren (2013) demonstrated that WV-2 is highly capable of identifying vegetation characteristics that influence biodiversity in grasslands; Takenaka et al. (2017) used VW-2 for the accurate detection and mapping of pine wilt disease; and Adam et al. (2017) successfully mapped *Prosopis glandula* using the WV-2 data.

Dimson (2017) used Species Distribution Models (SDMs) on temporally distributed data to detect the spread of invasion of PSHB in California. The results presented by Dimson (2017) identified areas most vulnerable to invasion and showed that SDMs were able to reliably detect PHSB infected trees. Additionally, Dimson (2017) highlighted the need for improving data both statistically and spatially in order to yield more accurate results on PSHB invasions and to overcome factors such as temperature bias.

Remote sensing, particularly the use of multispectral imagery such as WorldView-2, for the detection of *Fusarium Dieback* has not yet been fully explored. The image analysis techniques and machine learning used in remote sensing provide an opportunity to explore non-invasive approaches to detecting *Fusarium Dieback* and other stresses in trees before visible symptoms can appear, which could potentially save large populations of trees if detected early enough (Alonzo et al., 2014).

High spectral and spatial resolution remote sensing, such as WorldView-2, have evolved from the more moderate resolution sensors providing a new capability of distinguishing even the most minute differences in chemical and structural variations of tree species in order to map individual tree species in complex urban environments (Hartling, 2019).

2.8. Machine Learning techniques for tree species mapping

Machine learning are specialized statistical techniques that provide accurate and efficient processing capabilities for image classification, remote sensing, and data modelling (Shi, 2020). According to Shi (2020), machine learning is most promising for remote sensing of individual tree species, because it handles high dimensionality well; is capable of processing large datasets; and reduces variability and redundancy of data (Shi, 2020).

Several studies have shown and proven the reliability of machine learning algorithms (such as, among others; RF, SVM, neural networks, maximum likelihood) in mapping urban tree species and other vegetation successfully (Wichmann and Ravn, 2001; Verlic et al., 2014; Mutanga et al., 2012; Takenaka et al., 2017; Adam et al., 2017; Xulu et al., 2018; Abutaleb et al., 2020; Jombo et al., 2020). Furthermore, such techniques are becoming more commonly accessible, automated, and implementable making it easier to use and understand (Shi, 2020). Several open-source software exist for the use of machine learning applications that are highly favourable for remotely sensed data and image classification/segmentation processes, including, amongst others; R Studio, MatLab, Python, Statistica, etc. GIS and Remote sensing software such as ArcGIS, QGIS, and Erdas Imagine also have built-in tools and functions for machine learning processes that are highly accurate and widely used.

Machine learning has become a popular processing tool in remote sensing because of its capacity to identify spectral and structural variables from remote sensing datasets. Shi (2020) describes the capability of machine learning as having a “high exploratory power for differentiating among tree species” and establishing workflows for predicting outcomes (Shi, 2020: 113). Furthermore, the deterministic power of the machine learning algorithms coupled with its ability to classify and analyze multi classes of satellite data make it an optimal tool for detecting and mapping tree species and other vegetation (Shi, 2020). The statistical application of probability theory and the improved classification accuracies of land cover mapping has popularized machine learning as a fundamental part of remote sensing studies (Faithpraise et al., 2013).

CHAPTER 3:

Methodology

3.1. Study Area:

The city of Johannesburg is a metropolitan municipality located within the Gauteng Province of South Africa. It has a subtropical climate and an annual average rainfall of 750mm, with a warm summer from October to March, and a dry winter between early April and September (Naicker et al., 2003). The average daily temperature variations in the city can range between 16.6°C and 26.2°C (Abutaleb et al., 2020).

The City is a predominantly natural grassland biome. However, it still boasts one of the largest urban forests in the world with an approximation of about 10 million trees (Schäffler and Swilling, 2012). Because dominant and large forests are not common in grassland biomes, there is a visual contrast between the fast-growing urban forest of Johannesburg street trees and the surrounding natural grassland environment. This began sometime in the 19^{th} Century when the need arose to rid Johannesburg of dust and air pollution caused by mining (and the Gold Rush), which consequently led to the introduction of alien plant species into the city (Schäffler and Swilling, 2012). Several types of trees were planted, which are now dominant in the Johannesburg landscape, and among these are the London Plane, Jacaranda and Eucalyptus (Abutaleb et al., 2020).

This study was conducted in the northern suburbs (Parkhurst and Parktown North) of the City of Johannesburg (Fig. 4). Based on the field surveys conducted by Fryer (2019); Paap et al. (2019); and Van Den Berg et al. (2019) these suburbs were among the areas showing the greatest number of PSHB infestations within the city. Additionally, these suburbs are dominated by London Plane (*Platanus x acerifolia*) trees, both healthy and infested, making it an ideal site for this study. The two suburbs have shown a high rate of PSHB infestation compared to other Johannesburg suburbs, particularly along the Jan Smuts Avenue and Empire Road which are considered major thoroughfares running through the area. The main land use activity in the study area is residential, business, and public open space. This study focused on the London Plane tree species that were infested by PSHB in these suburbs, showing signs of *Fusarium Dieback infestation*.

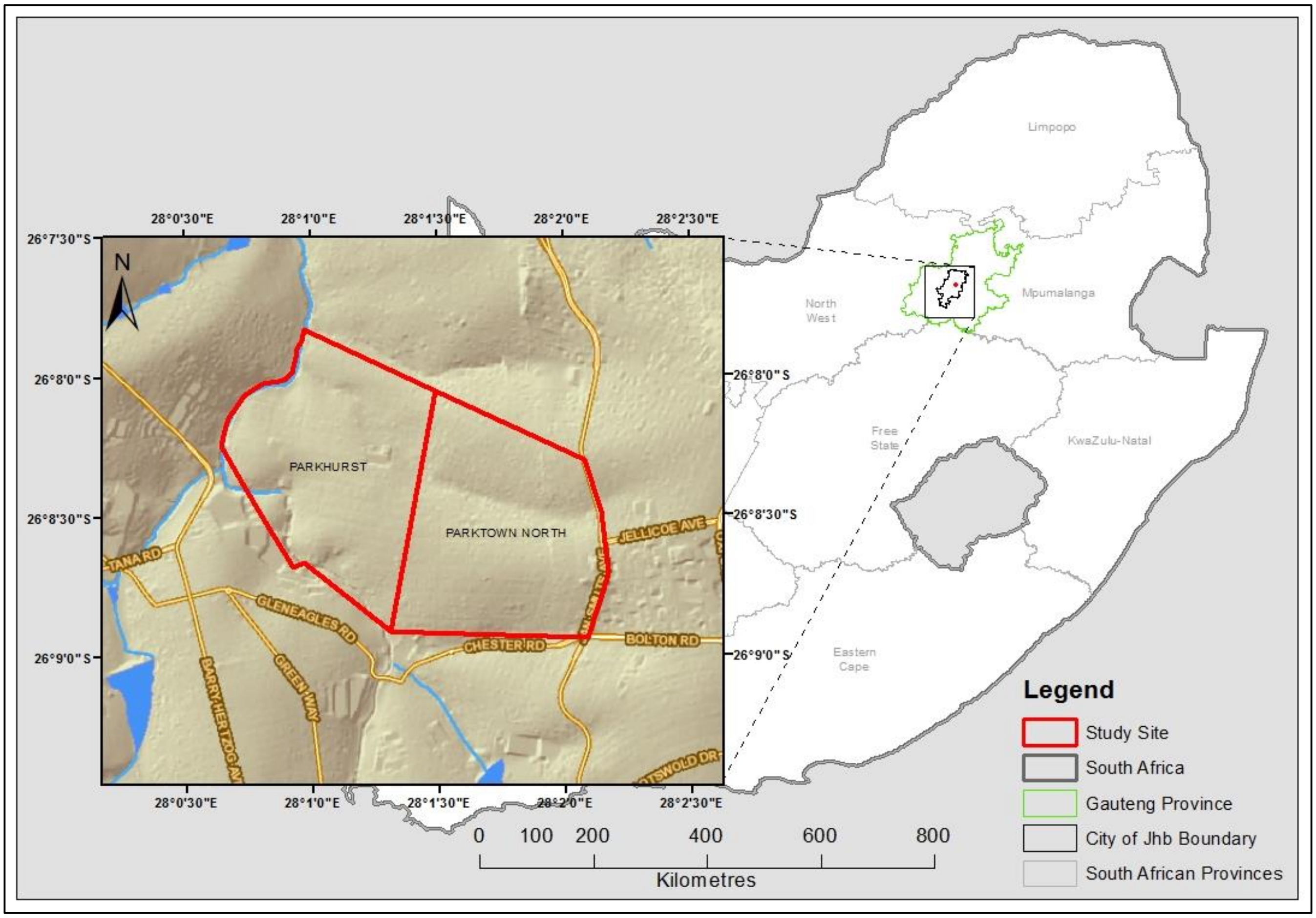

Figure 4: Location of the study area bounding Parkhurst and Parktown North suburbs in the city of Johannesburg, Gauteng

3.2. Image Acquisition and Pre-processing:

A WorldView-2 (WV-2) satellite image was used to map the distribution of the London Plane trees. The WV-2 multispectral satellite is a 2009 product of Digital Globe that records high resolution spectral and spatial signatures of plant species across eight different bands (Digital Globe, 2010). The study site was covered by one WV-2 scene acquired in November 2019 from the Corporate Geo-Informatics Directorate (Development Planning Department) at the City of Johannesburg Municipality. The 2m spatial resolution WV-2 image was captured under cloud-free conditions. The imagery is delivered geometrically and radiometrically corrected by the manufacturer (DigitalGlobe, 2010). No geometric, radiometric, or atmospheric corrections were done on the WorldView-2 product. All image pre-processing and orthorectifications were completed by the manufacturer (DigitalGlobe, 2010).

The WV-2 imagery consists of eight bands, as explained in table 1. These include the four standard bands (blue, green, red, and near-infrared (NIR)), and four new bands (coastal, yellow, near-infrared-2 (NIR-2), and red edge). The additional bands have enhanced classification accuracy at species level. The coastal band has led to improved chlorophyll detection; while yellowness detection has increased with the addition of the yellow band (Immitzer et al., 2012; Shojanoori and Shafri, 2016; Abutaleb et al., 2020). The NIR-2 band has proven useful in biomass studies; and the red edge band has become widely used in expanding the detection of vegetation stresses as well as species composition (Immitzer et al., 2012; Shojanoori and Shafri, 2016; Abutaleb et al., 2020). As such, all eight bands were used in the mapping of London Plane trees in Johannesburg for the specified study site.

Table 1: WorldView-2 spectral characteristics

WV-2 Band	Central Wavelength (nm)	Spectral Resolution (nm)	Spatial Resolution (m)
1 – Coastal	425	400-450	1.85
2 – Blue	480	450-510	1.85
3 – Green	545	510-580	1.85
4 – Yellow	605	585-625	1.85
5 – Red	660	630-690	1.85
6 – Red Edge	725	705-745	1.85
7 – NIR-1	833	770-895	1.85
8 – NIR-2	950	860-1040	1.85

3.3. Reference Data collection

The study site was first visited in March 2020 with professionals from Johannesburg City Parks and Zoo (JCPZ) who assisted in ensuring accurate identification of infested London Plane trees. The JCPZ professionals specialize in studying the *Fusarium Dieback infestation* and therefore provided pivotal information on infestation characteristics by which the infested trees could be identified. In addition to this, the site visit was used to identify the other major land-cover classes dominant within the area. A second site visit was done in January 2021 to confirm that infested trees were not removed from the study area, no major land cover changes occurred, and to collect additional data points. Site visits were not done in 2019 (at the same time as data acquisition) resulting in a gap period between image acquisition and data collection that could impact the data analysis and outcomes. This time lapse period between November 2019 and January 2021 may have resulted in healthy trees becoming infested; infested trees becoming more severely stressed with consequent mortalities; or even the removal of dead/infested trees from the study site. The reference datasets do not account for these possible changes and may therefore result in biased or inaccurate results. Two reference datasets were then compiled and named Reference Dataset 1 and Reference Dataset 2. For Reference Dataset 1, in addition to a London Plane tree species (LP) class, four other general land-cover classes were identified: (i) Other Tree Species (OT); (ii) Built-up Areas (BU); (iii) Grassland (GR); and (iv) Tar Road (TR). For Reference Dataset 2, the London Plane (LP) class was split into 2 classes – Healthy London Plane trees (HL) and Infested London Plane Trees (IL), to determine if the WV-2 bands could be used to distinguish between healthy and infested trees of the same species. Broadly characterized land-cover classes were used to group features that shared similar spectral characteristics and to avoid having multiple land-cover classes that could potentially create confusion in the final classification. Additionally, the focus of the study is on distinguishing infestation in trees and not at mapping the different land use in the study area. Table 2 describes the various land-cover classes, for both datasets, in more detail.

Table 2: Descriptions of the various land-cover classes used in the study

Class Name	Class Code	Class Description
London Plane	LP	London Plane trees

Other Trees	OT	Other tree species not identified as London Plane
Built-up Areas	BU	Roofing, houses, and other buildings or developments
Grassland	GR	Green open spaces, fields, and any area with bare grass or vegetation
Tar Road	TR	Streets, roadway, and tar surfaces
Healthy London Plane	HL	London Plane trees identified as healthy (i.e. without the presence of *Fusarium Dieback* infestation)
Infested London Plane	IL	London Plane trees identified as infested (i.e. showing the presence of *Fusarium Dieback* infestation)

The two reference datasets were used for this study, as described in tables 3 and 4. The reference data was used to compute confusion matrices for accuracy assessments per objective, and to train the classification algorithms. The two reference datasets (Reference Dataset 1 and Reference Dataset 2) were created from a combination of both primary (on-field data collection) and secondary (sourced from JCPZ's and Tree Survey's infestation database) data points. The in situ points for both datasets were collected through a non-random purposive sampling process. First, streets within the study area that were lined predominantly with London Plane trees had to be selected. This was done based on a visual assessment of the trees along the streets. No specific sampling method was used to do this. Once the main participating streets were chosen, a non-probability purposive sampling method known as homogeneity sampling was used to decide which tree points to capture. The homogeneity sampling method enabled the research to focus on creating a sample of trees that met the two main requirements: being a London Plane (*Platanus x acerifolia*) species; and showing signs of *Fusarium Dieback infestation*. For the infestation IL class in Reference Dataset 2, infested London Plane trees were selected based on visible evidence of *Fusarium Dieback infestation*, including PSHB presence, boring holes, sugar volcanoes, yellow/brown leaves, and varying amounts of branch die-back. London Plane trees that did not show signs of infestation were selected for the LP and HL classes of Reference Dataset 1 and Reference Dataset 2, respectively. Any London Plane tree identified on either side of the chosen streets were included in the datasets irrespective of any sampling pattern or transect. The locations of numerous trees, along all other streets, that were not London Plane species were captured and classified under the OT class. Spatial coordinates of each tree was recorded using a handheld Global Positioning System (GPS) device, Garmin eTrex 20 X.

Secondary data containing sample points of various infested tree species covering the northern Johannesburg suburbs was extracted from the databases provided by Tree Survey and JCPZ. The points in the Tree Survey database were a combination of tree locations captured by arborists, as well as tree locations that were captured by the public and sent to Tree Survey through a mobile application. Each entry included the species type of the tree captured. Points with a species type identified as London Plane were extracted from the database and used in the IL class. The JCPZ database did not contain any information captured by or received from the public. The sample points were collected by JCPZ professionals with specialized knowledge of field data collection and the *Fusarium Dieback infestation*. These points were considered more reliable than the in situ data or the Tree Survey dataset. The same process of extracting only infested London Plane tree species points was used and the selection extracted from the database for inclusion in the IL class. All other tree species appearing in the databases that fell within the study boundary was exported and used as part of the OT class. The various extracted sets of sample points were consolidated in ArcMap 10.2.2 and cleaned of any overlaps (in cases where points overlapped, the JCPZ point was used). Classes were then assigned accordingly. The WV-2 colour composite image and Google Earth satellite imagery were also used to identify points for the remaining land-cover classes, and to confirm the location of points that were placed on more than one pixel. Each class's points were captured at random intervals.

The Reference Dataset 1 had a total of 433 points across the five participating land-cover classes, which was randomly split into 70/30 training/test data, as shown in table 3 below.

Table 3: Composition of the 70% training and 30% test data for the different land-cover classes used in Reference Dataset 1

Reference dataset 1			
Classes	**Training Dataset (70%)**	**Test Dataset (30%)**	**Total**
BU	90	38	128
GR	60	25	85
LP	66	27	93
OT	32	13	45

TR	58	24	82
Total	306	127	433

For the second reference dataset, primary data points were collected in March 2020, January 2021, and March 2021 when infestation rates were expected to be at its highest and the symptoms of *Fusarium Dieback infestation* to be most spectrally visible. These points were used to create an additional land-cover class called Infested London Planes trees (IL) which served as the focal data of the study. The London Plane tree species class (LP) was replaced with a class called Healthy London Plane trees (HL). Thus, the second reference dataset contained four of the same land-cover classes as the first dataset, in addition to healthy London Plane trees (HL) and infested London Plane trees (IL). Dataset 2 had a total of 491 points across the six participating land-cover classes, which was randomly split into 70/30 training/test data, as shown in table 4.

Table 4: Composition of the 70% training and 30% test data for the different land-cover classes used in Reference Dataset 2

Reference dataset 2			
Classes	**Training Dataset (70%)**	**Test Dataset (30%)**	**Total**
BU	90	38	128
GR	60	25	85
OT	66	27	93
TR	41	17	58
HL	32	13	45
IL	58	24	82
Total	347	144	491

The distribution of the reference data across the study site is shown in Figure 5.

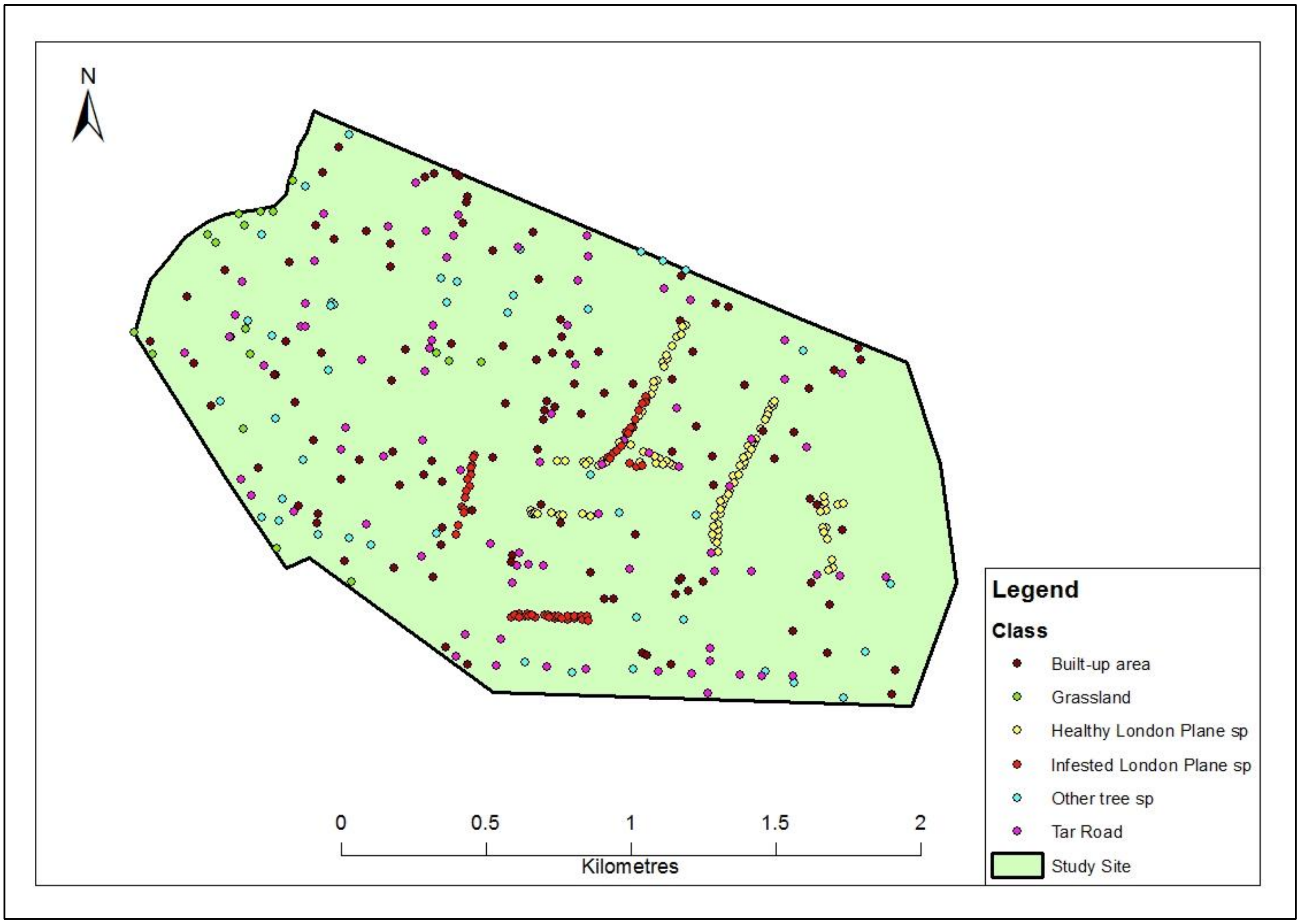

Figure 5: Distribution of the ground truth data per class collected in the study area, covering Parkhurst and Parktown North in the city of Johannesburg, Gauteng

3.4. Data Analysis and Image Classification

The Random Forest (RF) and Support Vector Machines (SVM) algorithms were used to classify the WV-2 imageries. The statistical software package R, version 3.6.3., was used for all data analysis and image classification processes, as well as for the accuracy assessments. These machine learning classifiers were chosen for the image classification processes because they have been widely credited as super-performers in vegetation mapping studies (Abutaleb et al., 2020) and have proved advantageous in tree species mapping of heterogeneous and complex urban environments (Jombo et al., 2020).

Random Forest (RF) and Support Vector Machines (SVM) have both been praised for their reliability, as well as the advantage of accurate predictions using small training samples (Thabeng et al., 2019). These supervised, pixel-based image classification techniques were both used in this study to first map the London Plane street trees against other tree species and land-cover classes; and thereafter to distinguish between healthy and infested London Plane trees and other land-cover classes. For each objective, the RF and SVM classifiers were trained using the 70% training sample, and tested for accuracy using the 30% test sample data.

Random Forest is a supervised classification method based on creating unpruned decision trees using subsets of the training dataset, most commonly selected by random sampling with replacement from an original dataset (Mutanga et al., 2012). The RF model creates a forest of decision trees (classification trees in this case) to assign categorical values (e.g. land-cover class types such as forest-1, grass-2, water-3, etc.) to each pixel in an image based on the majority vote of the decision trees in the forest, until a classified image of predicted values is created. Because RF is an ensemble model, it incorporates results generated from several models (in this case, multiple decision trees) to calculate a response rather than relying on the outcomes of a single prediction (Horning, 2010). The bootstrapping, random selection process is only done on the training dataset – that is, only using two-thirds of the original observations or reference dataset, leaving one-third of the reference dataset (referred to as "out-of-bag" or OOB samples) to be used for estimating the classification error and testing the model accuracy of the overall prediction (Thabeng et al., 2019).

Specific parameter requirements in the algorithm include *mtry* (number of predictor variables used at each node split) and *ntree* (number trees to be grown in a forest) for which default values are calculated by the algorithm. According to Shi (2020), these are the two main parameters in Random Forest that control the accuracy of the classification. The *ntree* default value is set at 500, but can be increased if the number of trees required for the prediction accuracy (and low error rate) is not sufficient (Shi, 2020). The *mtry* default value is the square root of the number of variables used in the study (sqrt (n_features)) (Thabeng et al., 2019). For this study, a 10-fold cross validation search method was applied to tune the RF parameters. The 10-fold cross validation search method is a tuning technique in the *randomForest* package that computes the optimal parameter values by dividing the training data into 10 independent subsets, called folds (Shi, 2020). In addition to parameter tuning, the RF algorithm has the capability to compute valuable information about errors, Variable Importance (VI), and outliers in the data (Horning, 2010). This study will therefore analyze the VI measurement computed in the RF algorithm in order to understand which predictor variables (i.e. WV-2 bands) most significantly impacted the classification. For this study the

Mean Decrease Accuracy (MDA) measurement was used for determination of variable importance of the WV-2 bands in distinguishing infested London Plane trees.

Support Vector Machines (SVM) is a non-parametric and non-linear supervised machine learning algorithm used for data classification analysis (Abutaleb et al., 2020). SVM performs classification by calculating or finding the hyper-plane segregating classes, i.e. SVM is the coordinate or locality of the boundary between classes (Abutaleb et al., 2020). The aim of SVM is to determine the best hyper-plane for segregating the various classes resulting in a better performing classification of objects at the pixel level (Jombo et al., 2020). Like RF, the SVM algorithm uses a sample from the reference data to determine the value of the rest of the population data. Thus, it assigns classes to the unknown pixels based on the most representative known training samples, or support vectors, closest to the optimal hyper-plane, thereby also minimizing the threshold of classification errors (Abutaleb et al., 2020).

The concept of linear separability through an optimal hyper-plane in a 1-dimensional space is explained in the Figure 6.

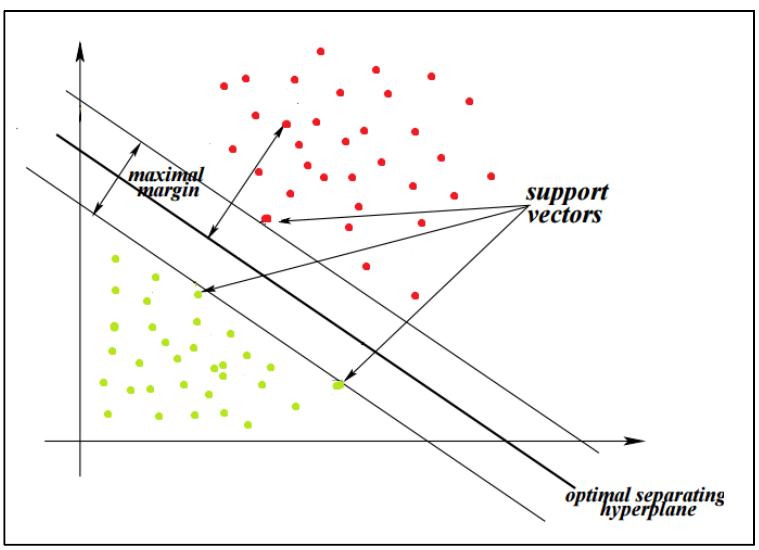

Figure 6: Determination of the optimal hyper-plane, maximum margin, and support vectors in SVM

This study used the SVM kernel functionality, Radial Basis Function (RBF), because of its known success in mapping various land-cover classes as well as different tree species (Jombo et al., 2020). The SVM RBF function was applied with the eight WV-2 bands in order to determine the best hyper-plane for classifying the various land-cover classes, and London Plane species. SVM classification for this study was done using the *e1071* package in the R software. RBF kernel function needs the tuning of two particular hyper-parameters in order to achieve higher levels of classification accuracy - “cost” (C) and "gamma" (γ) (Zafari et al., 2017). The Cost (C) function is used to determine the minimal amount of loss that can be accepted without compromising on accuracy of the classification, more commonly understood as the cost of misclassification. The gamma parameter (γ) determines the spread or width of the kernel and aims to establish the most effective fit of the hyper-plane in nonlinear classification problems. For this study, a 10-fold cross-validation (previously explained) was used to tune the cost and gamma parameters which determined the parameter combination with the lowest error to train the algorithm.

3.4.1. Accuracy Assessment

An accuracy assessment is used to compare the classified image to another data source (usually ground-truthing points) in order to determine how accurately the classification algorithm performed (Morales-Barquero et al., 2019). Abutaleb et al. (2020) describe the accuracy assessment as a determination of the accuracy with which the results closest resemble the value accepted as true. As such, it identifies if the pixel in the satellite imagery that were ground truthed have been classified correctly or not (Abutaleb et al., 2020).

In order to assess the accuracy of the classified images, 30% of the reference datasets were compared to the classified image in confusion matrices. The confusion matrices were used to compute different accuracy metrics including the Overall Accuracy (OA), User's Accuracy (UA), and Producer's Accuracy (PA) in order to evaluate the reliability of the RF and SVM classifiers on a WV-2 imagery (Morales-Barquero et al., 2019).

A kappa analysis using the *k* statistic was also calculated in each confusion matrix, showing the degree of agreement wherein a kappa coefficient of 1 (or close to 1) indicates perfect agreement (Morales-Barquero et al., 2019). A kappa coefficient of 0 indicates that there is no agreement between the classification and the ground truthed pixel (Abutaleb et al., 2020).

All accuracy assessments were conducted in R software package.

CHAPTER 4:

Results

4.1. Mapping London Plane Tree Species

The first objective of this study was to determine if WV-2 can accurately distinguish the London Plane tree species from other tree species and land-cover classes. This was tested using the two classifiers, RF and SVM, to determine which of the two algorithms will more accurately and effectively classify London plant trees from the rest of the LULC classes. The final results indicate that both RF and SVM classifiers were able to identify and classify London Plane trees from other land-cover types with RF (87.40% accuracy and 0.8363 kappa) performing marginally better than SVM (86.61% and 0.8259 kappa).

4.1.1. Parameter Optimization for Random Forest

The RF algorithm optimizes the best *ntree-mtry* parameter combination by cross-validating *ntree* values of between 500 and 9500 (at 1000 intervals) with *mtry* values of between 2 and 8, as indicated in the RF optimization table below. The results of the 10-fold cross-validation sampling method for parameter tuning showed that the best values for the *ntree* and *mtry* parameters were 1500 and 4, respectively, as shown in table 5 and figure 7. Combining these parameter values resulted in the lowest OOB error rate of 15.35% (this is shown by the yellow highlighted field in table 5). This is a generally well accepted OOB percentage to be produced since low OOB error values indicate a high performance of the Random Forest classifier. Thus, the *ntree* value of 1500 and the *mtry* value of 4 were used to train the RF algorithm for distinction of London Plane tree species from other land-cover types.

Table 5: RF optimization of ntree and mtry parameters in a 10-fold cross-validation

mtry values	ntree values									
	500	1500	2500	3500	4500	5500	6500	7500	8500	9500
2	0.1598925	0.1565591	0.1565591	0.1565591	0.1565591	0.1565591	0.1565591	0.1565591	0.1565591	0.1565591
3	0.1600000	0.1600000	0.1566667	0.1566667	0.1598925	0.1598925	0.1566667	0.1598925	0.1598925	0.1598925
4	0.1666667	0.1534409	0.1534409	0.1598925	0.1566667	0.1632258	0.1632258	0.1598925	0.1598925	0.1632258
5	0.1665591	0.1633333	0.1633333	0.1666667	0.1698925	0.1665591	0.1666667	0.1698925	0.1665591	0.1634409
6	0.1665591	0.1633333	0.1666667	0.1698925	0.1666667	0.1731183	0.1666667	0.1698925	0.1731183	0.1731183

	7	0.1666667	0.1764516	0.1731183	0.1764516	0.1698925	0.1732258	0.1666667	0.1698925	0.1731183	0.1731183
	8	0.1698925	0.1764516	0.1698925	0.1763441	0.1764516	0.1764516	0.1698925	0.1763441	0.1732258	0.1764516

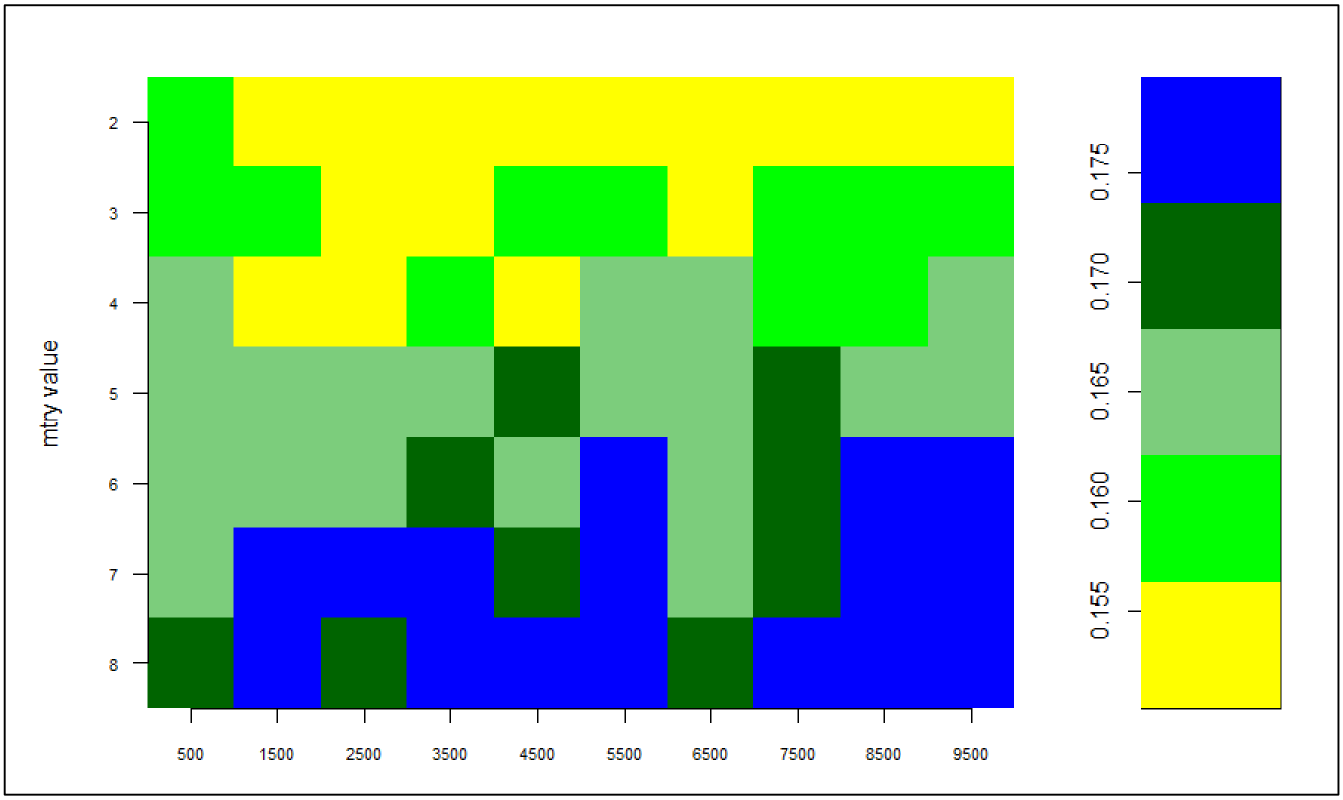

Figure 7: Optimization of Random Forest parameters (*ntree* and *mtry*) outcome from using a 10-fold cross-validation method for a WorldView-2 image

4.1.2. Variable Importance (VI) measurement

The RF algorithm determined the relative importance of each WV-2 band in the classification process, as shown in figure 8. The VI measurement was used to determine which variables are the most influential for the classification process. The Variable Importance of each WV-2 band in the RF classification procedure was calculated using the Mean Decrease Accuracy (MDA). The highest MDA indicates the most essential bands required for the best possible classification outcome. The variables, in this study, were the eight WV-2 bands (costal, blue, green, yellow, red, red edge, NIR-1 and NIR-2). The most important bands for WV-2 determined by the RF classifier were B5 (Red), B4 (Yellow), and B8 (NIR-2). B3 (Green) performed the lowest in the MDA analysis, followed by B2 (Blue), and B7 (NIR-1).

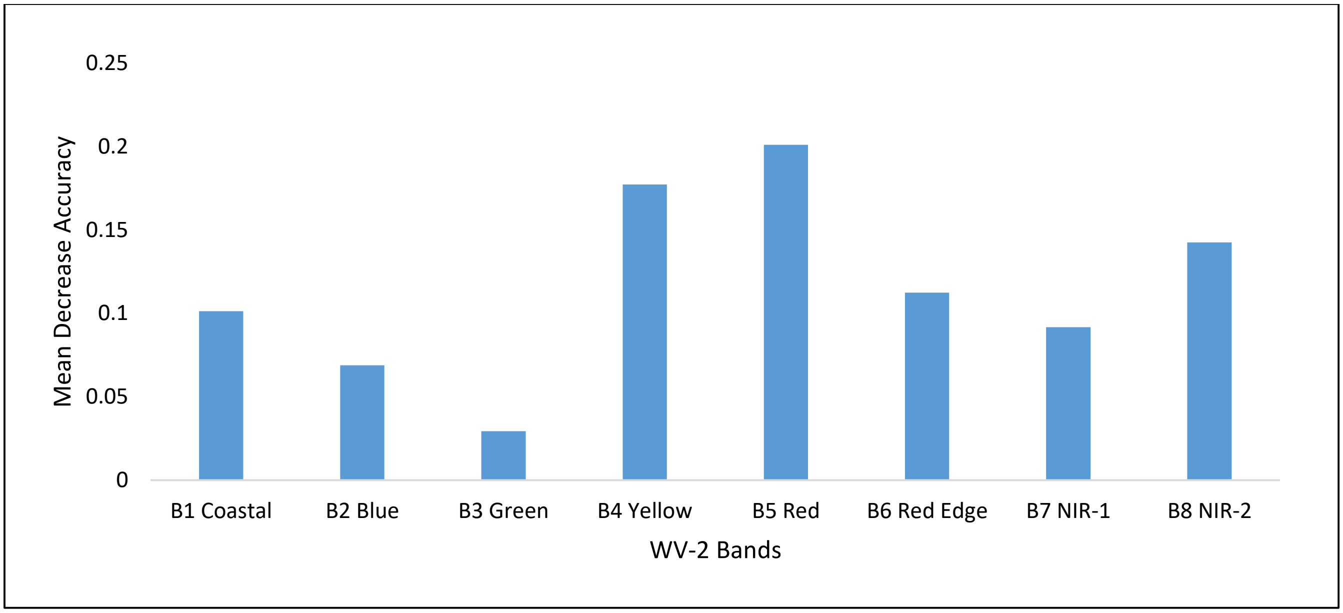

Figure 8: Relative importance of each WV-2 band in the overall classification process as determined by the RF classifier by measurement of Mean Decrease Accuracy values per band

All 8 bands in the WV-2 image were included in the VI measurement for each class in the study. The VI measurement, by determination of uppermost MDA values, determined which bands were most essential for mapping each of the land-cover classes, as shown in Figure 9. The results indicated that for mapping the London Plane tree species (LP), the most necessary bands were B5 (Red), B8 (NIR-2), and B1 (Coastal). Similarly, the most important band for the grassland class (GR) was B8, B5, and B7. For the Other Trees class (OT) all bands obtained low MDA values, with the values for B2, B3, and B5 being negative. These negative MDA values indicated that the variable negatively impacts the classification accuracy. Additionally, the negative values indicate that there was a negative relationship between OT and the other classes in the study. B8 performed best for the OT class. Thus, for all the vegetation-related classes (i.e. London Plane trees, Other Trees, and Grassland) B8 were identified as important for classification. The NIR bands have been previously identified as being pivotal in the classification of individual tree species (Jombo et al., 2020).

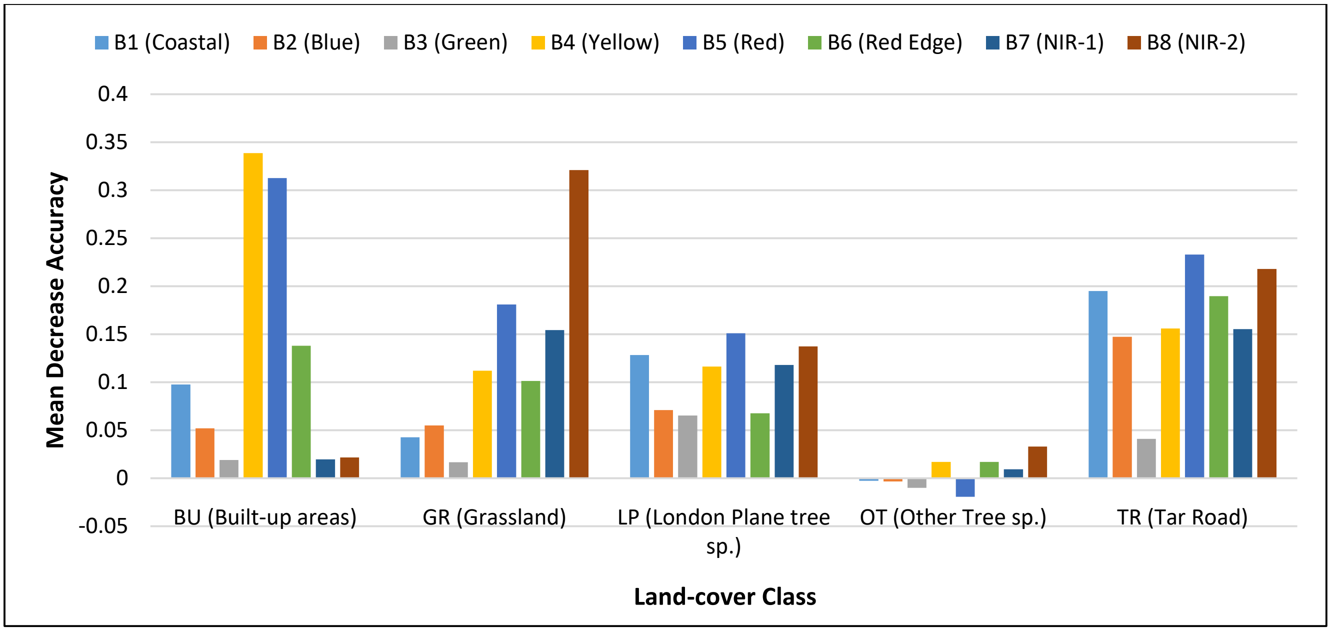

Figure 9: Relationship between predictor variables (WV-2 bands) and each land-cover class based on Mean Decrease Accuracy values calculated per band per class

4.1.3. Parameter Optimization for Support Vector Machines

The 10-fold cross-validation technique determined the best gamma (γ) and cost (C) parameter values for the RBF kernel SVM algorithm to yield optimal accuracy in classification. As such, the best γ and C values were 1 and 10, respectively, as shown in Figure 10. The best performance at this parameter combination yielded the lowest error rate of 15.65% and were therefore used to train the SVM algorithm.

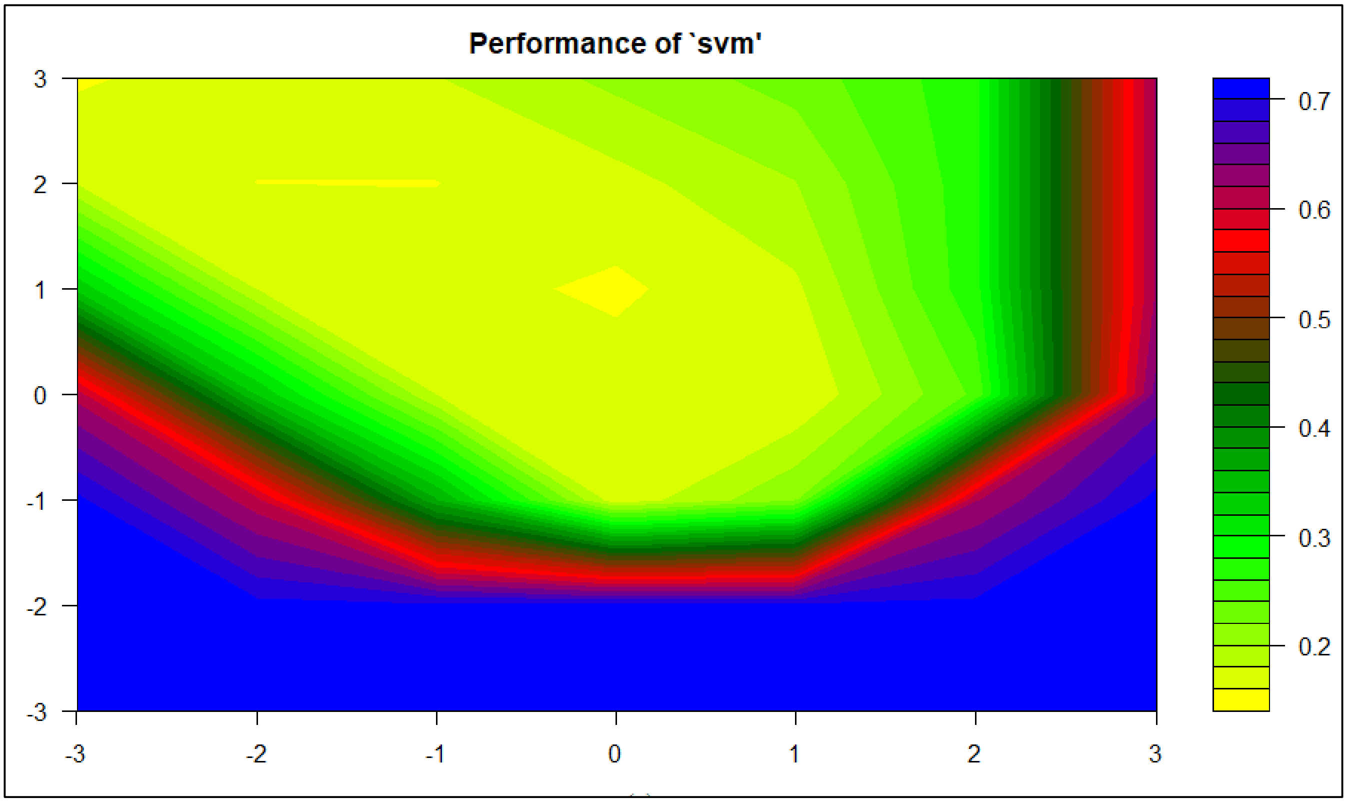

Figure 10: Optimization of SVM parameters (γ and C) outcome from using a 10-fold cross-validation method for a WorldView-2 image

4.1.4. Accuracy Assessment

The 30% test data from Reference Dataset 1 was used to assess how well RF and SVM performed in classifying London Plane tree species and other land-cover types using the WV-2 imagery. The test dataset contained a total of 127 instances that participated in the accuracy assessments for both RF and SVM classifiers. The classification accuracies were tested by means of employing confusion matrices. Various accuracy metrics were analyzed in the confusion matrices, discussed below.

The results of the accuracy assessment derived from the confusion matrix for the RF algorithm is shown in table 6. The User's Accuracy (UA) for the different classes ranged from 72.22% to 100%; while the Producer's Accuracy (PA) ranged from 7.69% to 100%. The UA was lowest on the London Plane tree species class (72.22%) and highest on the Other Trees class (100%), while the PA was the lowest on the Other Trees class (7.69%) and highest on the Grassland class (100%). For this part of the study, the focus class is LP. As such, the confusion matrix indicated that 26 of the 27 LP class instances were correctly classified, with a PA of 96.30%. This means that only 1 omission error occurred – 1 LP instance was incorrectly classified as GR class. 10 Commission errors were identified in the confusion matrix. These were instances of the OT class that were classified as LP, thus contributing significantly to the LP class's UA (72.22%). Only 1 instance of the OT class was correctly classified while the other 12 were classified as LP (10) and BU (2). All other classes had PA values over 94%.

The Overall Accuracy (OA) was 87.40% wherein 111 instances of the total 127 were correctly classified across all classes in the test dataset. A kappa coefficient of 0.8363 (83.63%) was achieved by the RF classifier.

Table 6: Confusion matrix for RF in mapping London Plane trees and other land-cover classes

Random Forest Confusion Matrix									
Classified Data	Reference Data								
	Class	BU	GR	LP	OT	TR	Diagonal Total	Row Total	UA
	BU	36	0	0	2	1		39	92.31%
	GR	0	25	1	0	0		26	96.15%
	LP	0	0	26	10	0		36	72.22%
	OT	0	0	0	1	0		1	100.00%
	TR	2	0	0	0	23		25	92.00%
	Column Total	38	25	27	13	24	111	127	
	PA	94.74%	100.00%	96.30%	7.69%	95.83%			
	OA	87.40%							
	kappa coefficient	0.8363							

The results of the accuracy assessment derived from the confusion matrix for the SVM algorithm is shown in table 7. The User's Accuracy (UA) for the different classes ranged from 0% to 96.15%; while the Producer's Accuracy (PA) ranged from 0% to 100%. For both UA and PA, the lowest performing class was OT where no instances were correctly classified, thus having 0% in both cases. Of the 13 OT class instances, 11 were misclassified as LP and 2 as BU. The LP class had 26 correctly classified instances; only 1 omission error where LP was classified as GR; and 11 commission errors where OT was classified as LP. Thus, the LP class had a PA of 94.74% and a UA of 70.27%. All other classes had PA values over 94% with the exception of the OT class. The Overall Accuracy (OA) achieved was 86.61% with 110 of the total 127 instances correctly classified across all classes. A kappa coefficient of 0.8259 (82.59%) was achieved by the SVM classifier.

Table 7: Confusion Matrix for SVM in mapping London Plane trees and other land-cover classes

SVM Confusion Matrix									
Classified Data	Reference Data								
	Class	BU	GR	LP	OT	TR	Diagonal Total	Row Total	UA
	BU	36	0	0	2	1		39	92.31%
	GR	0	25	1	0	0		26	96.15%
	LP	0	0	26	11	0		37	70.27%
	OT	0	0	0	0	0		0	0.00%
	TR	2	0	0	0	23		25	92.00%
	Column Total	38	25	27	13	24	110	127	
	PA	94.74%	100.00%	96.30%	0.00%	95.83%			
	OA	86.61%							
	kappa coefficient	0.8259							

4.1.5. Spatial distribution of London Plane trees and other land-cover classes

The classification maps shown in figures 11 and 12, are outputs of the RF and SVM classification processes, respectively, and show the final classification and spatial distribution of the London Plane trees and other land-cover classes in the study site. Both classifiers were able to map the different classes with relative accuracy and consistency, except for the Other Tree species (OT) class which were classified poorly in both outputs. In the RF classification map, there is visual evidence of the OT class being sparsely distributed across the study site, while there is even less evidence of the OT class in the SVM map. This was in contrast to the expectation that OT would be the dominant land-cover type since it is a representation of the different and densely populated street trees known to exist within the study site. Consequently, almost all instances of street trees in both classification maps were classed as London Plane tree species (LP), implying that the majority of trees in the study site were London Plane, with very little heterogeneity among the species of trees that exist within the area. Tar Roads, Built-Up areas, and Grasslands were clearly classified in both maps, with high degrees of accuracy.

The inset maps of both figures 11 and 12 show how similarly the RF and SVM classifiers performed, and clearly depicts the dominance of the LP class's spatial distribution across the study site. The inset maps also illustrated that the RF classifier was able to better classify BU and OT classes than SVM (this can be seen by little visibility of brown (BU) and orange (OT) symbols in the SVM inset) for that particular part of the study area. Overall, both algorithms were able to successfully map the spatial distributions of London Plane trees and the other land-cover classes with good accuracy.

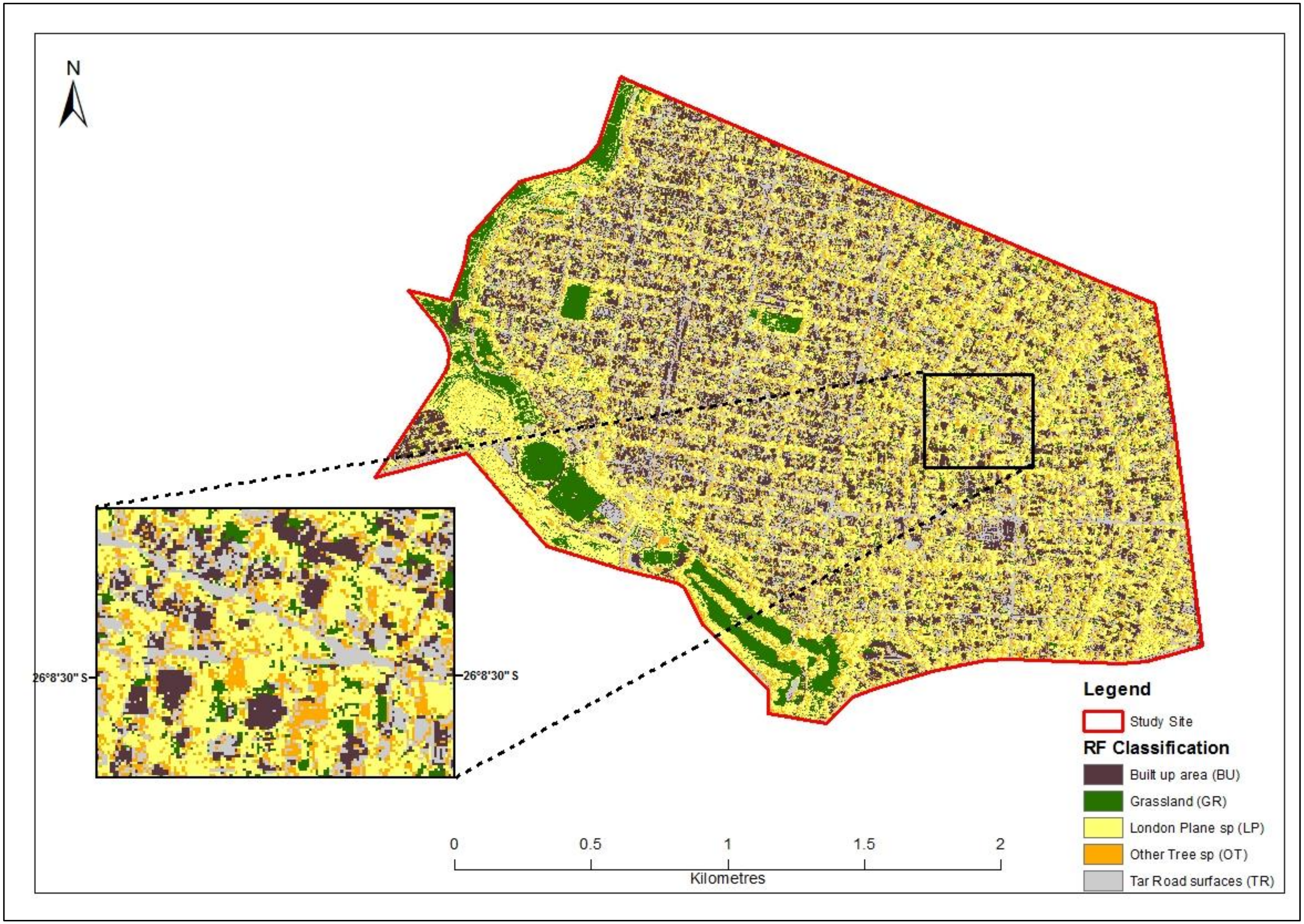

Figure 11: Spatial distribution of London Plane trees and other land-cover classes in the final classification map computed by the Random Forest algorithm

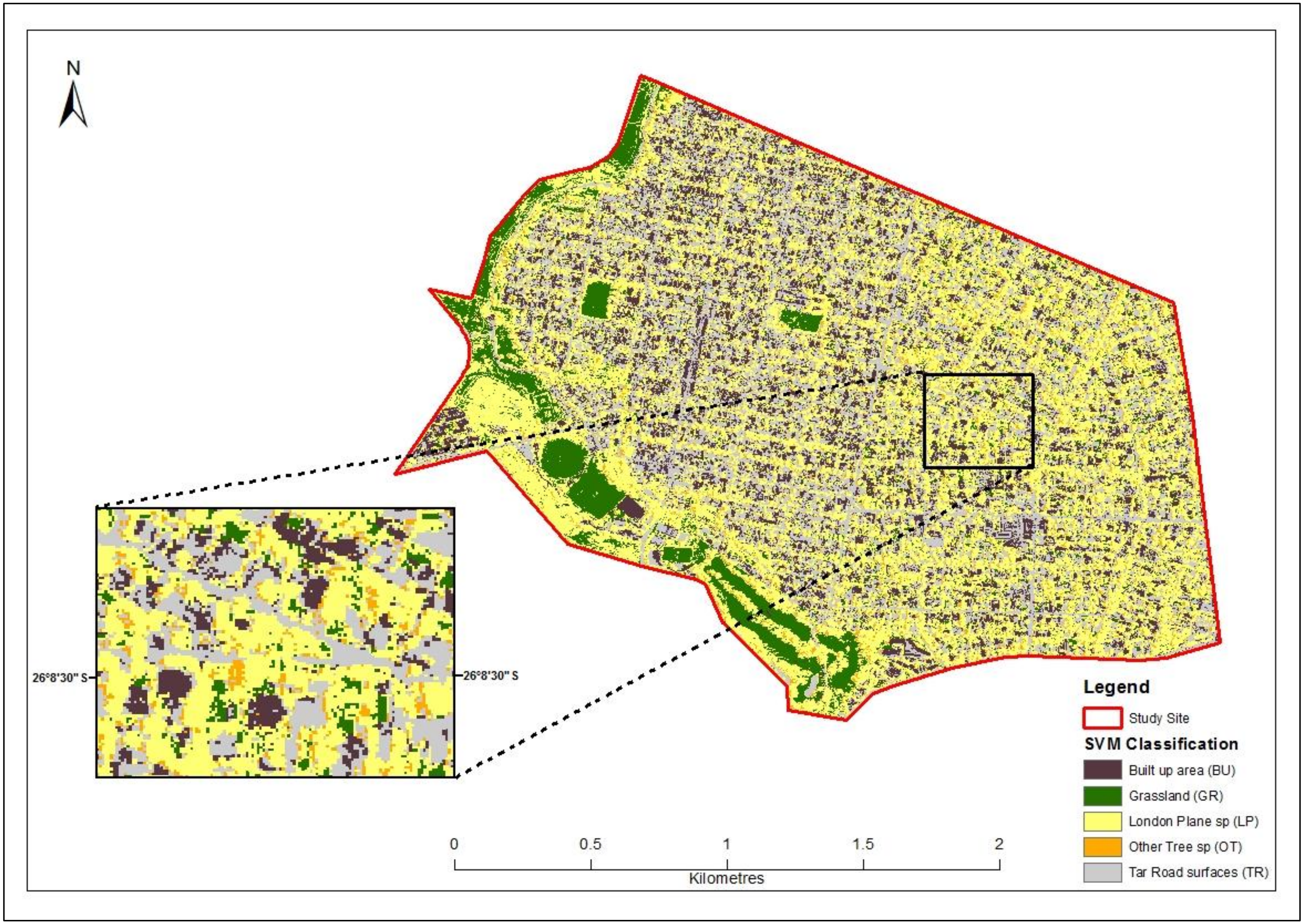

Figure 12: Spatial distribution of London Plane trees and other land-cover classes in the final classification map computed by the Support Vector Machines algorithm

4.2. Mapping London Plane tree species infested with *Fusarium Dieback* infestation

Subsequent to the successful identification of the London Plane tree species in the outcomes above, this study also set out to evaluate the utility of the WV-2 image in discriminating between healthy and infested trees of the same tree species, London Plane. This was also done using both RF and SVM algorithms to determine which algorithm has a higher performance power in detecting *Fusarium Dieback* on London Plane trees. This objective was undertaken using the same process as previously but with a different input dataset. Reference dataset 2 was used to obtain the results and classification maps discussed below. The final results indicate that both RF and SVM classifiers were not able to correctly distinguish London Plane trees infested with *Fusarium Dieback* from the healthy London Plane trees. For both classifiers, the overall accuracy achieved was 75%.

4.2.1. Parameter optimization for Random Forest

The results of the 10-fold cross-validation parameter optimization showed that the best values for the *ntree* and *mtry* parameters were 3500 and 2, respectively, as shown in table 8 and Figure 13. The lowest OOB rate for this parameter combination was 27.92% (this is shown by the yellow highlighted field in table 8). Thus, the *ntree* value of 3500 and the *mtry* value of 2 were used to train the RF algorithm for distinction of infested London Plane trees from healthy London Plane trees and other land-cover types.

Table 8: RF optimization of ntree and mtry parameters in a 10-fold cross-validation

		ntree values									
mtry values		**500**	**1500**	**2500**	**3500**	**4500**	**5500**	**6500**	**7500**	**8500**	**9500**
	2	0.290924	0.285126	0.282185	0.279244	0.282269	0.282185	0.285126	0.279244	0.279244	0.285126
	3	0.290840	0.287983	0.285210	0.288067	0.285126	0.285126	0.285126	0.285126	0.285126	0.285126
	4	0.288067	0.290924	0.290840	0.282269	0.285210	0.285126	0.279328	0.282269	0.279328	0.285126
	5	0.299832	0.296807	0.288151	0.282353	0.293950	0.291008	0.288151	0.296807	0.293950	0.288235
	6	0.299748	0.302605	0.299748	0.293866	0.305462	0.288151	0.293866	0.291092	0.296807	0.291008
	7	0.299580	0.313950	0.296723	0.291008	0.291008	0.291008	0.288151	0.293950	0.296807	0.291008
	8	0.296723	0.305378	0.302437	0.305294	0.299664	0.296723	0.302437	0.302521	0.299580	0.293866

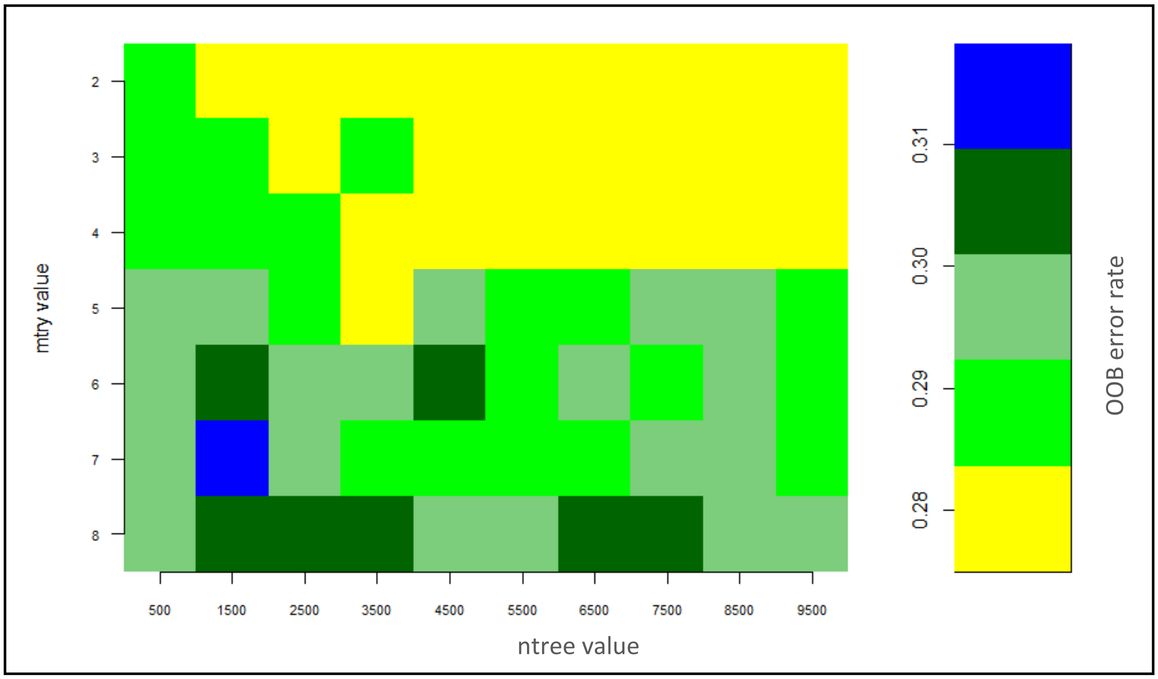

Figure 13: RF optimization of *ntree* and *mtry* parameters in a 10-fold cross-validation

4.2.2. Variables Importance (VI) measurement

As can be seen in Figure 14, the most important spectral band measured by the RF algorithm in the VW-2 dataset for the second part of the study was also B5, the Red band. This was followed by bands B4 (Yellow), B8 (NIR-2), and B6 (Red Edge). B3 (Green) and B7 (NIR-1) performed the lowest in the MDA assessment.

The most important bands for Healthy London Plane (HL) class was B1 (Coastal), B5 (Red), and B4 (Yellow). For the Infested London Plane trees class (IL) the most important bands were identified as B6 (Red Edge), B3 (Green) and B7 (NIR-1), as shown in figure 14. For the other classes, the most important bands were B4 for BU, B8 for GR, B1 for the OT class, and B8 for the TR class. Bands 2, 3, and 7 obtained negative MDA values for the OT class, similar to the findings of the previous objective. This reinforces the suggested reasons discussed in the previous section – the OT class negatively impacts the classification accuracy, and shared a negative relationship with other variables in the study. The negative MDA values also suggest a high bias and error margin for the WV-2 bands with the OT class. All tree species related classes (HL, IL, and OT) had extremely low MDA values for all bands compared to the remaining land-cover types (BU, GR, and TR).

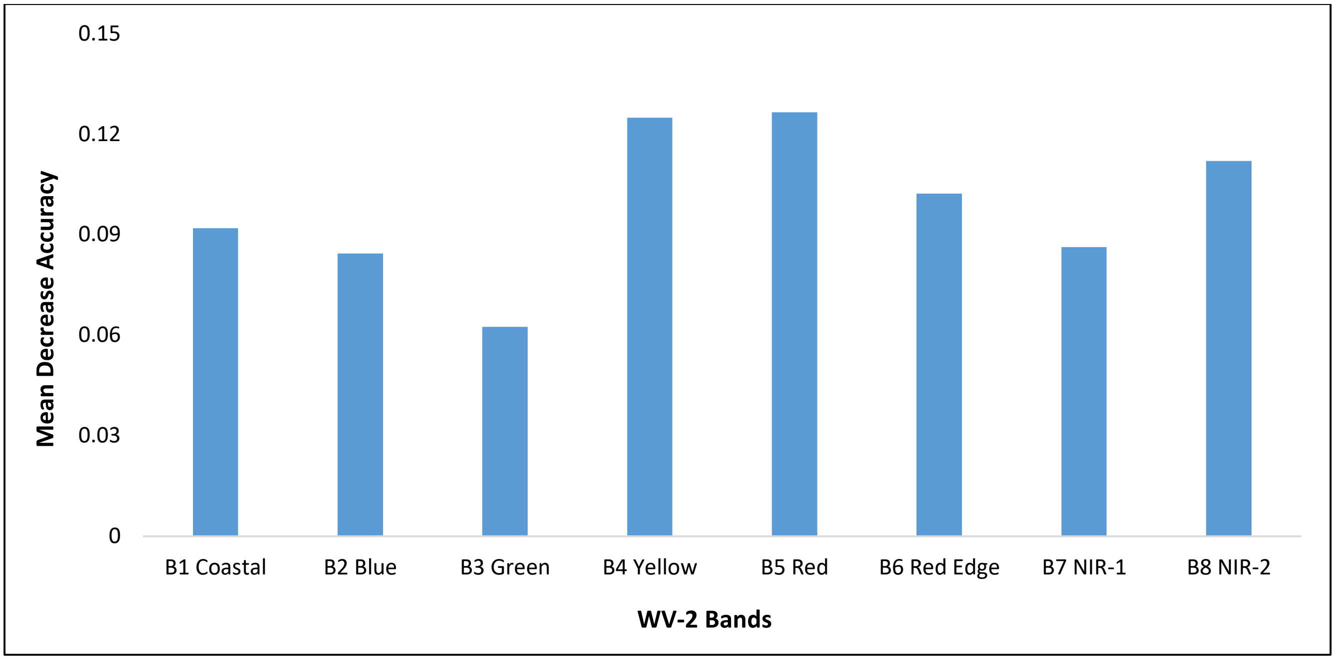

Figure 14: Relative importance of each WV-2 band in the overall classification process as determined by the RF classifier by measurement of Mean Decrease Accuracy values per band

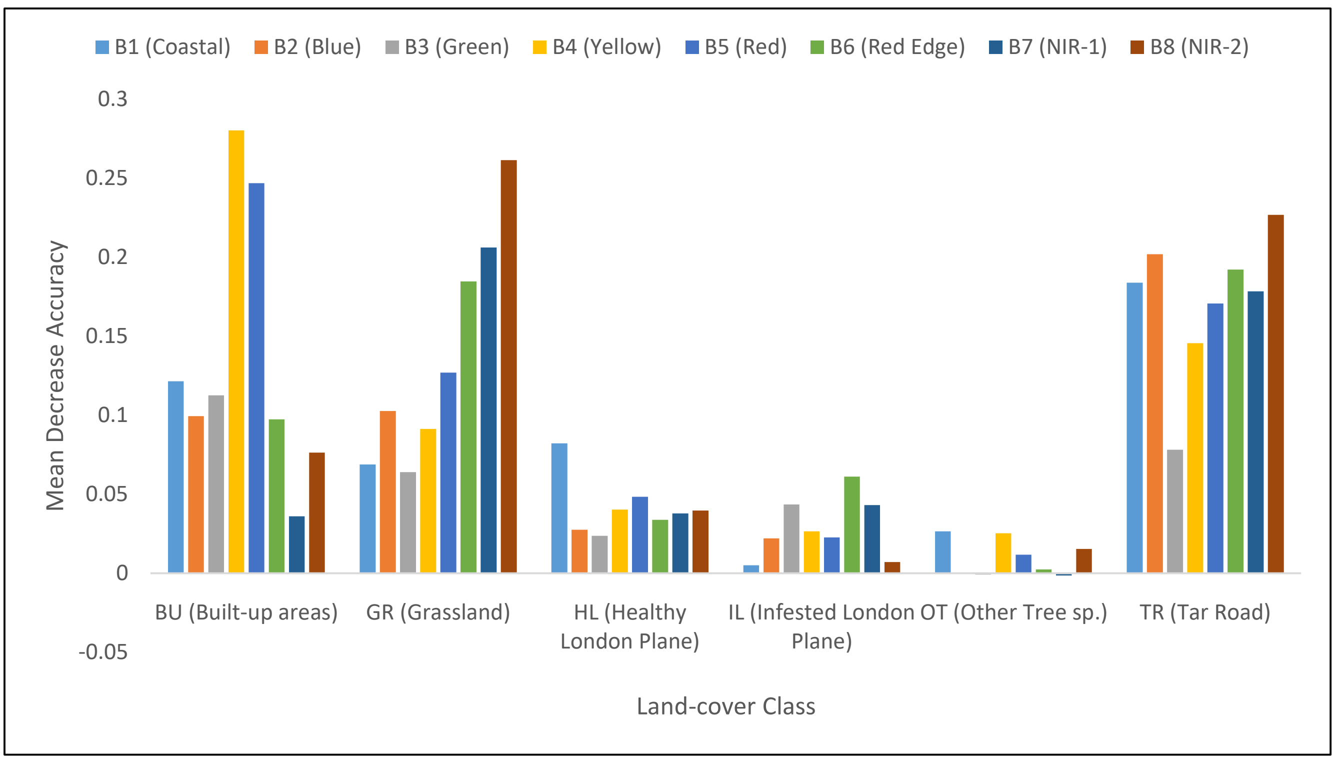

Figure 15: Relationship between predictor variables (WV-2 bands) and each land-cover class based on Mean Decrease Accuracy values calculated per band per class

4.2.3. Parameter Optimization for Support Vector Machines

For the second part of the study, the optimal parameter combination was once again determined and subsequently used to train the SVM algorithm. The best gamma (γ) and cost (C) parameter values determined by the 10-fold cross-validation technique were 0.1 and 10 respectively, as shown in figure 16 below. The lowest OOB error of 25.64% was achieved from this parameter combination.

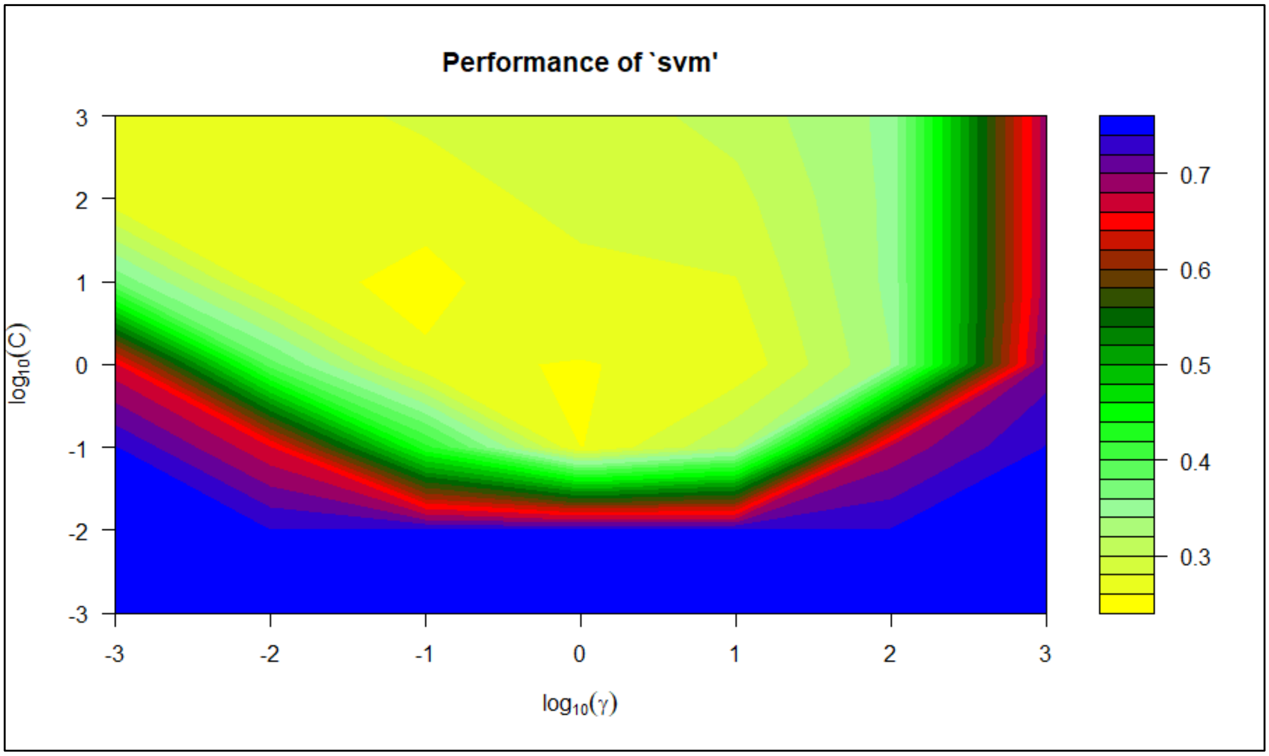

Figure 16: SVM optimization of γ and C parameters in a 10-fold cross-validation technique for WV-2

4.2.4. Accuracy Assessment

The test data from Reference Dataset 2 was used to assess how well RF and SVM performed in distinguishing between healthy and infested London Plane trees and other land cover types using the WV-2 imagery. The test dataset contained a total of 144 instances that participated in the accuracy assessment. The various accuracy metrics are discussed in the confusion matrices.

The results of the accuracy assessment confusion matrix for the RF algorithm is shown in table 9. The User's Accuracy (UA) ranged from 33.33% to 92.59%; while the Producer's Accuracy (PA) ranged from 7.69% to 100%. The UA was lowest on the Other Trees (OT) class (33.33%) and highest on the Grassland (GR) class (92.59%), while the PA was also lowest on the OT class (7.69%) and highest on GR class

(100%). For this part of the study, the focus class is IL – London Plane trees infested with *Fusarium Dieback* infestation. As such, the confusion matrix indicated that only 7 of the 17 IL class instances were correctly classified, with a PA of 41.18%. This means that 10 omission error occurred in the classification of infested London Plane trees constituting more than half of the total IL instances – 1 IL instance was incorrectly classified as OT class while 9 instances were misclassified as HL. 12 Commission errors were identified in the confusion matrix for the IL class. These were 5 instances of the OT class that were classified as IL, 1 instance of TR, and 6 instances of the HL class. Only 1 instance of the OT class was correctly classified while the other 12 were classified as BU (2), HL (3), IL (5), and TR (2).

The Overall Accuracy (OA) was 75% wherein 108 instances of the total 144 were correctly classified across all classes in the test dataset. A kappa coefficient of 0.6909 (69.09%) was achieved by the RF classifier. Based on these values, the RF algorithm appeared to have a low performance in classifying the Infested London Plane trees. Much of the confusion or misclassification occurred between the HL, IL, and OT classes, indicating that the RF algorithm performed poorly in distinguishing between tree classes. The other classes (BU, GR, and TR) performed well in the accuracy assessment. This showed that RF had the capability to accurately classify different land-cover classes, but encountered a high degree of error for distinguishing between healthy and infested London Plane trees from other tree species in this study. The OA statistic was increased by the performance of the other land-cover classes' performance in the accuracy assessment, whereas HL, IL, and OT classes performed considerably lower. The kappa coefficient is above average, but indicates that the overall performance of the classification was only slightly better than a random classification.

Table 9: Confusion matrix for RF in distinguishing infested London Plane trees and other land-cover classes

Random Forest Confusion Matrix										
		Reference Data								
Classified Data	Class	BU	GR	HL	IL	OT	TR	Diagonal Total	Row Total	UA
	BU	36	0	0	0	2	2		40	90.00%
	GR	0	25	2	0	0	0		27	92.59%
	HL	0	0	18	9	3	0		30	60.00%
	IL	0	0	6	7	5	1		19	36.84%
	OT	0	0	1	1	1	0		3	33.33%
	TR	2	0	0	0	2	21		25	84.00%

	Column Total	38	25	27	17	13	24	108	144	
	PA	94.74%	100.00%	66.67%	41.18%	7.69%	87.50%			
	OA	75.00%								
	kappa coefficient	0.6909								

The results of the accuracy assessment derived from the confusion matrix for the SVM algorithm is shown in table 10 below. Generally, the SVM algorithm performed lower than the RF algorithm in the accuracy assessment. The User's Accuracy (UA) for the different classes ranged from 0% to 96.15%; while the Producer's Accuracy (PA) ranged from 0% to 100%. For both UA and PA, the lowest performing classes were IL and OT where no instances were correctly classified, thus having 0% in both cases.

Of the 13 OT class instances, 8 were misclassified as HL, 1 as IL, and 4 as TR. The HL class had 26 of the 27 correctly classified instances; only 1 omission error where HL was classified as GR. For the IL class, the SVM classifier was not able to accurately classify any of the instances correctly wherein all 17 were misclassified as HL. 1 OT and 1 TR instance were misclassified as IL. This shows that the SVM algorithm struggled with differentiating the Infested London Plane trees from other tree species, but was able to identify and classify Healthy London Planes trees with high accuracy.

The Overall Accuracy (OA) achieved was 75% with 108 of the total 144 instances correctly classified across all classes, exactly as the RF classifier performed in this case. However, unlike the RF classifier, the SVM classifier was not able to distinguish any IL or OT instances correctly. Its overall performance was enhanced by the correct classification of the other land-cover types, particularly the HL class. A kappa coefficient of 0.6874 (68.74%) was achieved by the SVM classifier, performing slightly lower than the RF algorithm in the accuracy assessment.

Table 10: Confusion matrix for SVM in distinguishing infested London Plane trees and other LULC classes

SVM Confusion Matrix										
Classified Data		**Reference Data**								
	Class	**BU**	**GR**	**HL**	**IL**	**OT**	**TR**	**Diagonal Total**	**Row Total**	**UA**
	BU	36	0	0	0	0	2		38	94.74%
	GR	0	25	1	0	0	0		26	96.15%
	HL	0	0	26	17	8	0		51	50.98%
	IL	0	0	0	0	1	1		2	0.00%

	OT	0	0	0	0	0	0		0	0.00%
	TR	2	0	0	0	4	21		27	77.78%
	Column Total	38	25	27	17	13	24	108	144	
	PA	94.74%	100.00%	96.30%	0.00%	0.00%	87.50%			
	OA	75.00%								
	kappa coefficient	0.6874								

It is conclusive to state that both classifiers performed almost the same in the accuracy assessment with RF performing slightly better than SVM, indicated by the small difference in kappa. Both classifiers had problems in differentiating infested London Plane trees from the healthy London Plane and other tree species, but were able to classify other land-cover classes with a high level of accuracy. Infested London Plane trees were classified poorly for both classifiers, but performed better with the RF algorithm.

4.2.5. Spatial distribution of Infested London Plane trees and other land-cover classes

The classification maps shown in figures 17 and 18, are outputs of the RF and SVM classification processes, respectively, and show the final classification and spatial distribution of the Infested London Plane trees and other land-cover classes in the study site. These classification maps are of particular importance to this study as it is an indication of both algorithm's ability to distinguish London Planes trees infested with the *Fusarium Dieback* disease within the study area when combined with the 8-band WV-2 image.

The classification map generated from the WV-2 image with the RF classifier indicates that there was widespread dispersion of infested London Plane trees across the study area. There was no particular area that the infestation was concentrated to. Both outputs showed a dominance of the Healthy London Plane tree class, implying that the majority of street trees are of London Plane species and not the heterogeneity that the area is known for. Both classifiers were able to map the BU, GR, and TR classes with high accuracy and consistency. The Other Tree species (OT) class was classified poorly in both outputs, with very little visual evidence of this class. This is in contrast to the expectation that OT would be the dominant land-cover type since it is a representation of the different and densely populated street trees known to exist within the study site.

The inset maps of both figures 17 and 18 show clearly the differences of the two classifiers when combined with the WV-2 image. The area represented in the inset maps is a region of the study site where high infestation was expected to occur (as suggested by the ground-truth data collected at the start of this study). However, both maps indicate that the infestation is evenly distributed across the study site, with the RF classifier assigning IL class to more pixels than the SVM classifier. Both inset maps clearly illustrated the dominance of the LP class's spatial distribution across the depicted region.

Overall, both classification maps indicated a failure to correctly map the spatial distributions of *Fusarium Dieback* infestation on London Plane trees among the other land-cover classes.

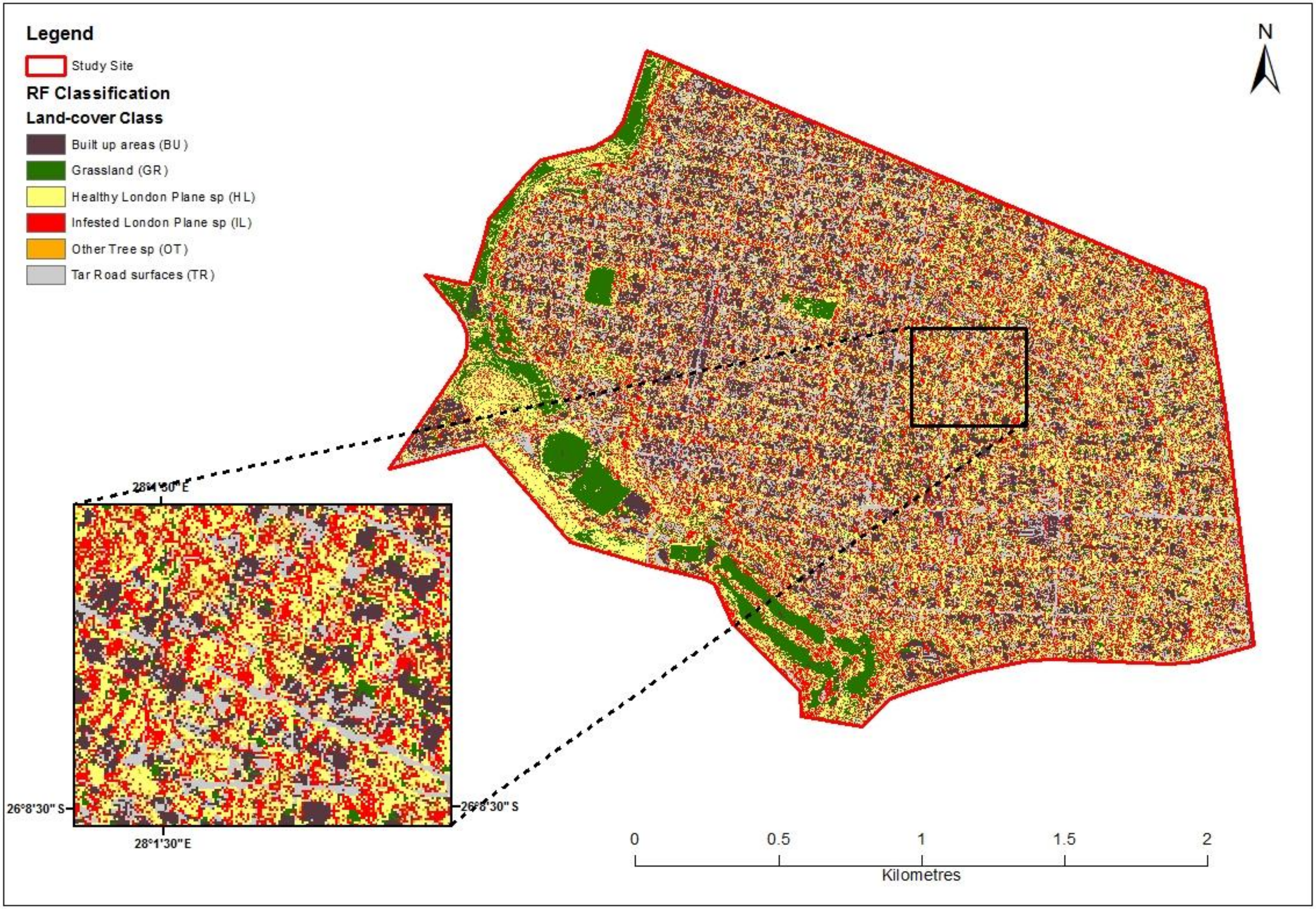

Figure 17: Spatial distribution of Infested London Plane trees and other land-cover classes in the final classification map computed by the Random Forest algorithm

Figure 18: Spatial distribution of Infested London Plane trees and other land-cover classes in the final classification map computed by the Support Vector Machines algorithm

CHAPTER 5:

Discussion

This study sought to evaluate the performance of the multispectral, high-resolution remote sensing WV-2 satellite imagery using the Random Forest (RF) and Support Vector Machines (SVM) classification algorithms for effective discrimination of London Plane tree species infested with the *Fusarium Dieback* infestation from healthy London Plane trees, as well as other tree species and land-cover classes, in the northern suburbs of Johannesburg, South Africa. To do this, the first objective addressed whether or not London Plane tree species (i.e. irrespective of health status) can be distinguished from other tree species and land-cover types. This was done using the RF and SVM algorithms to determine if the classification accuracy would change when the WV-2 image is combined with different high-powered classification algorithms. The second objective further separated the London Plane tree species according to its health status (i.e. healthy – no presence of the *Fusarium Dieback* infestation; or infested – definite presence of the *Fusarium Dieback* infestation) to determine if the WV-2 image can correctly and accurately identify the *Fusarium Dieback* infestation on London Plane trees. This was tested using both RF and SVM classifiers to determine if one algorithm performed better than the other in distinguishing between individual tree infestations at a species level.

5.1. Mapping London Plane Trees Species

The performance of the WV-2 image in the two classification processes showed overall results of high accuracy for both RF (87.40% with kappa 0.8363) and SVM (86.61% with kappa 0.8259) when mapping London Plane trees against other land-cover types. This was largely attributed to the increased number of spectral bands in the WV-2 image that provided the opportunity for spectral distinction between London Plane tree species and other tree species that exhibit quite similar spectral characteristics. Thus, this study indicated that individual tree species, such as the London Plane trees, can accurately be identified at the species level in complex urban environments. The findings in this study is in agreement with other studies that have proven the effectiveness of WV-2 data in urban tree species mapping (Mutanga et al., 2012; Abutaleb et al, 2020; Jombo et al., 2020; Stohlgren, 2010).

Both classification maps (RF and SVM) obtained high user's and producer's accuracies for all classes except the Other Tree (OT) class where most of the misclassifications occurred. This indicated a high degree of spectral confusion between the OT and London Plane (LP) classes due to pixel mix-up. One of the reasons for this low accuracy in classifying the OT class could be due to a result of imbalanced or disproportioned data in the test dataset (i.e. there were more LP than OT instances that participated in the accuracy assessment). The test dataset contained 27 LP points but only 13 OT points, suggesting an uneven distribution of instances between the two tree-type classes. The presence of such a class imbalance can severely skew the final class vote (Nasi et al., 2018). Additionally, Nasi et al. (2018) postulated that models that have been trained on unbalanced datasets tend to perform poorly when they are required to generalize. As such, the higher prevalence of LP than OT in the models may have caused the algorithms to categorize data in the majority class thus failing to identify the minority class. Nasi et al. (2018) have shown that imbalanced datasets negatively impact classification accuracies and must be compensated for in the algorithm being used (e.g. employing minimization cost functions for each class; assigning different weighting methods for each class based on their representation in the dataset; or resampling the dataset through either undersampling the majority class or oversampling the minority class).

Another reason that the two classes were not well discriminated from one another could be because all tree species used in the reference datasets that were not classed as London Plane were grouped as Other Trees. Thus, the datasets could contain trees species of the greater *Platanus* genus in the OT class that should have been in the LP class due to phytomorphological similarities with London Plane, thereby resulting in greater spectral confusion among the tree classes. Jombo et al. (2020) reported spectral confusion between London Plane trees and at least 5 other tree species, to varying degrees, causing minor misclassifications in the overall accuracy results. Abutaleb et al. (2020) also postulated that grouping too many woody vegetation types (such as different tree species) into one class with only one species in another class (that study used Eucalyptus while this study used London Plane) can result in biased data with inaccurate classifications as a result of pixel mix-up, and anatomical and morphological properties that several tree species share. Other researchers also highlighted similarities among several tree species as a main cause of mixed pixels and misclassifications in their studies (Alonzo et al., 2014; Gudex-Cross et al., 2017; Li et al., 2015; Liu et al., 2017; Zhang and Qiu, 2012).

5.2. Mapping London Plane Tree Species infested with *Fusarium Dieback* Infestation

In the second part of the study, when mapping infested London Plane trees against healthy London Plane trees, other tree species, and land-cover types, both classification processes obtained a result of 75% with RF (kappa 0.6909) and SVM (kappa 0.6874). This finding is consistent with the very similar research done by Immitzer and Atzberger (2014) in which they tested the applicability of WV-2 in distinguishing bark beetle infestations with an outcome of 75% overall accuracy. Other studies detecting bark beetle and pest-related infestations on urban forests with the use of moderate to high resolution sensors, and other remotely sensed imagery, performed far lower: Abdullah et al. (2019) achieved 67% accuracy with Sentinel-2 and 36% with Landsat-8; Marx (2010) obtained 51% using RapidEye, and Nasi et al. (2014) achieved 73% using a combination of various UAV datasets.

While both algorithms resulted in the same overall accuracy, RF performed marginally better than SVM, as indicated by the slightly higher kappa value. Both classification maps (RF and SVM) show clearly that the models did not succeed at accurately mapping the spread of the *Fusarium Dieback* infestation across London Plane trees within the study area. The drastic drop in accuracy levels and kappa values between the two objectives of this study, for both algorithms, indicates a failure to distinguish the *Fusarium Dieback infestation* with high accuracy, irrespective of which algorithm was used. This failure could be attributed to the limitations set out in the methodological approach of the study. First, the discrepancy between the time of the image acquisition (2019) and the date of data collection (2020/2021) leaves a considerable time gap. As such, the reference data collected will not correspond to the WV-2 image if major changes have taken place on the ground during this time lapse (e.g. healthy trees become infested, tree mortality rises, tree removals have taken place, etc.). Second, the field survey design used in this study was not scientifically sound enough to avoid inaccuracies in the datasets that were created. The purposive sampling method was prone to a considerable degree of researcher bias – streets were chosen based on visibility of London Plane trees rather than using a probable or random sampling technique (such as a horizontal or zigzag transect) which limited the number of trees being sampled and the distribution of those threes. The infested London Plane trees were clustered along a few streets, negating large regions of the study area. The proportion of the tree population that is made up by London Plane species in the study area is unknown which means that if the London Plane species only accounts for a scant fraction of the total population (<10%) then statistically significant conclusions will not be drawn.

Additionally, the results indicated that WV-2 imagery exhibited increased spectral confusion when trying to separate infested trees from healthy trees of the same species. Furthermore, there were several pixel mix-ups between Healthy London Plane trees (HL), Infested London Plane Trees (IL) and Other Tree species (OT), which corresponds to the results of the previous objective of this study, further reinforcing the notion that woody or tree-type species exhibit several similarities that cause mixed and misclassified pixels. This could be an accurate representation of the ground, however, this would suggest that almost all trees within the study area are London Plane (*Platanus × acerifolia*) species; and/or are infested with *Fusarium Dieback*. This does not correspond with the site visits conducted at the start of this project. The classification map generated from the WV-2 image with the SVM classifier indicated a similar result, but with less infested trees dispersed across the study site. Gairola et al. (2016) suggest that creating additional classes to represent the dominant woody species in a region, rather than grouping them all into one class (such as the OT class), will considerably lower spectral overlap among tree species that share similar spectral signatures. The tree species present in the HL, and OT classes likely share similarities in foliar morphology, phenological characteristics, and overlapping canopy cover, that make them spectrally indistinguishable from one another, thereby explaining the class mix-up. According to Gairola et al. (2016), post-classification processing would be a valuable solution to improving the quality of classifications in studies where the complexity of biophysical conditions and spectral confusion is prevalent.

The misclassifications of the IL class as OT can also be attributed to the data within the OT class that was extracted from the JCPZ and TreeSurvey databases. During this step, any tree species not categorized as infested London Plane was labelled as OT. This was done irrespective of the health status. Hence, trees of other species that were infested with *Fusarium Dieback* was included in the OT class. If those infested trees shared the same visible symptoms as the infested London Plane trees, and therefore also emitted the same spectral signature, then this could have serious implications in the classification process. Additionally, the study did not use a scale of infestation severity (i.e. mild, moderate, severe, and dead) when choosing how to categorize infestation. As a result, not all London Plane trees that were marked as infested would exhibit the same degree of visible symptoms, nor would they all be spectrally distinct. As such, healthy London Plane trees and trees only mildly infested (i.e. a low level of infestation, still in early stages of dieback) could still appear as quite similar and may not be detectable through remote sensing. Furthermore, trees experiencing stress and dieback from other factors (not *Fusarium Dieback*) were not considered or accounted for in this study. Those symptoms are not unique to severe *Fusarium Dieback infestation*. Consequently, those trees could be presenting similar symptoms to trees infested with *Fusarium Dieback* thereby contributing to the misclassification and spectral mix-up.

The reference dataset for this objective suffers the same bias of unbalanced data, as in the previous objective, but in this case both the OT and IL classes present themselves as minority classes, with OT having only 13 points in the test dataset, IL having only 17 points, while HL had 27. Several researchers have indicated that adding more ground-truthing data to the models considerably increases the classification accuracy and boosts the overall model performance (Carlotto, 2009; Jombo et al., 2020; Radoux et al., 2010; Stohlgren, 2010). Adjusting the bias and variance levels of the training and test data has also been postulated as a solution to data-related errors in classification (Radoux et al., 2010). In particular, errors of underfitting (i.e. inadequate representation of some classes of data in the relationship between actual and predicted values) are caused by high bias, while errors of overfitting (i.e. training data fits the model perfectly, but fails to classify unseen data) are caused by high variance in datasets that need to be more thoroughly reviewed before the classification process can be reiterated (Radoux et al., 2010).

In addition to the reasons already highlighted in this paper, the failure to correctly distinguish *Fusarium Dieback* infestation could be a result of several contributing factors. Firstly, there is the possibility of inaccuracies in the ground truth data that become detrimental in causing the misdetection of infestation in the classification processes. If the GPS coordinates of the infested trees were captured incorrectly during the data collection process, then the pixels in the image corresponding to those coordinated tree points will be incorrect and therefore mismatched (Carlotto, 2009). In addition to this, other research on plant-pests have shown that using health classes (i.e. healthy, infested, dead, etc.) without any focus on other land-cover classes have resulted in higher classification accuracies (Fassnacht et al., 2014; Nasi et al., 2018; Senf et al., 2017). Both Fassnacht et al. (2014) and Nasi et al. (2018) mapped the presence of bark-beetle-related infestation in trees with improved accuracies when using a two or three health class approach in combination with high resolution imagery.

Secondly, phenological characteristics necessary for the spectral and spatial identification of *Fusarium Dieback* may have changed between the time of data collection and the time of image capture. This means that London Plane trees showing presence of infestation at the time of data collection may have changed due to climate sensitivity, phenological cycles, or even the physical removal of the tree after the WV-2 image was captured and therefore the image is not a true reflection of the ground. Carlotto (2009) suggests the same in his research on the relationship between ground truth errors and low classification accuracies. Biochemical changes (such as chlorophyll content and nitrogen amounts) in leaves cause a change to spectral characteristics detectable by the various spectral bands. Depending on which stage of infestation the tree is at, and the rate of change of the biochemical properties during the infestation period, the spectral properties of the trees used in the reference dataset could have drastically changed, resulting in the reduced detection of the infestation at different wavelengths and spectral bands (Immitzer and Atzberger, 2014).

Thirdly, and most importantly, the characteristics/symptoms associated with the *Fusarium Dieback* infestation are not clearly distinguishable from other, similar, infestations and ecological stresses, through remote-sensing applications. While research has indicated that pest-related plant disease can be identified accurately with high-resolution remote sensors, there is also the challenge of symptom similarity (Fassnacht et al., 2014; Nasi et al., 2018). Quite a few insect diseases found in trees (such as the variations of *Fusarium Dieback* caused by different bark beetles) present with the same or similar symptoms that make it difficult to diagnose the infestation as being clearly one or the other. For example, infestations associated with bark beetles (insects similar to the Polyphagous Shot Hole Borer) all cause yellowed leaves, branch dieback, defoliation, etc. which can be detected by high-resolution remote sensing. As such, the existence of other tree infestations in the study site could have been misclassified as Infested London Plane (IL) trees in the study, resulting in the widespread distribution of the IL class in the classification maps. Furthermore, several species of trees in the study area are sensitive to climate variation and ecological stresses. This means that during the time of this study, trees suffering from the impacts of climate, ecological and other pre-existing stresses may have been misidentified as being infested with the *Fusarium Dieback* infestation thereby causing further confusion in the separability of infested, healthy, and other tree species. Symptoms indicating the infestation status of the London Plane trees were driven largely by borer holes present on the bark of trees, discoloration and staining on branches, and beetle galleries detectable inside the vascular system of the tree. As such, these properties are not visible or detectable by remote sensors. Because the branches and trunks of trees are usually covered by the foliage of leaf abundance they tend to have low reflectance values and do not receive as much visibility as a tree canopy would. Immitzer and Atzberger (2014), as well as Nasi et al. (2018), have shown that using crown discolouration, defoliation, and the well-lit parts of canopy cover as identifiers of bark beetle infestations result in high accuracy classifications.

The limitations of using a pixel-based approach for the classification of insect diseases has also been mentioned as a contributing factor to low accuracy outcomes. Nasi et al. (2018) indicate that using a tree-level-based approach instead of a pixel-based approach could drastically change the overall outcomes of image classification with high spatial resolution images. It is further postulated by their findings that multispectral imaging at the individual tree level is better done with the use of a central coordinate representing each tree in an image than classification per pixel. Similarly, Liu and Zia (2010) suggested a shift in scientific approaches away from pixel-based methods toward an object-based approach in order to overcome key limitations and drawbacks in the study of plant-pest relations and tree infestations at a species level.

5.3. Variable Importance of each WorldView-2 band

For both objectives of this study, the RF Variable Importance measurement index showed that the additional four bands in the WV-2 were favourable for mapping the London Plane trees, both healthy and infested. Of particularly importance was the red (B5) and NIR-2 (B8) bands. This aligns with the findings of Abutaleb et al. (2020) that the new bands in the WV-2 product enhance the classification of tree species in urban environments.

Overall, B5 was the most important band in both objectives, followed by B4 and B8. For almost all classes, B4, B5, and B8 reflected well and featured as a necessary variable for the reflectance of each class. The exception was the HL class which reflected best on the B1 Coastal band and least on B8. High water content in healthy leaves suggest a reason for the importance of B1 in this class (Immitzer and Atzberger (2014). The standard four bands (B1 to B4) had varying contribution to the reflectance and performance of the different land-cover classes. B1, B2 and B3 made little meaningful contribution to the overall classification; however, B4, the Yellow band, appeared to play an important role in class separability, featuring as the second most important band for both objectives and per class.

The “new” bands in WV-2, B5 to B8, played a more significant role in class separability, with B5 being the most influential class overall. These bands make up the SWIR (short wave infra-red) region and the findings here correspond with findings in other research for tree species mapping: According to Jombo et al. (2020) bands in the SWIR region are better suited to distinguish variations in biochemical content, moisture content, and changes in cellulose content of foliage. Alonzo et al. (2014) alluded that the SWIR region is ideally suited for separability of tree species and are successfully for classifying trees.

There was no consensus on one influential band among the tree classes. However, the HL and OT class both showed B1 as the most important band for classification. The IL class reflected best on B6, the Red Edge band, with low reflectance on B1. All three tree-classes reflected relatively well on B4 and B8, with varying reflectance values on bands 5, 6, and 7.

5.4. Summary

Based on the analysis of the study's results, and discussions on the key findings and associated challenges proposed here, this study concludes the following:

- The fine spatial and increased spectral properties of 8-band high-resolution WV-2 image is vital for urban tree species mapping, and was able to identify and map London Plane tree species with very high accuracy using both RF and SVM algorithms.
- In detecting London Plane tree species from other land-cover types, the WV-2 image performed better with the RF algorithm, generating a higher overall accuracy and kappa coefficient than SVM.
- In distinguishing between healthy and infested trees of the same species, the WV-2 image performed poorly with both algorithms (both achieved 75% overall accuracy), and failed to accurately identify the *Fusarium Dieback* infestation in London Plane trees.
- Consequently, this study finds that the algorithms are equally powerful and can therefore be chosen by preference when researching pest-related infestation in individual tree species.
- The accuracy obtained from WV-2 for distinguishing infested trees from healthy trees was not high enough to be considered successful, however, a 75% accuracy is considered a fairly good performance when comparing studies with lower resolution images that have performed with less than 75% accuracy (Abdullah et al., 2019; Marx, 2010). Thus, this study shows that the potential exists for using WV-2 satellite data in detecting PSHB attacks.
- The bands 4 (Yellow), 5 (Red), 6 (Red Edge) and 8 (NIR-2) were the most influential WV-2 bands in distinguishing healthy and infested London Plane trees, and other land-cover classes. Overall, B5 was the most important band. Thus, this study showed that the additional 4 bands in the WV-2 image are necessary for plant-pest disease mapping and contribute to increased class separability in complex urban forests.
- For this study, the SVM algorithm was chosen as the more appropriate classifier as the final classification map generated by SVM appears to be a truer reflection of the ground than the RF output, and due to SVM's ability to handle small test datasets better than RF.
- The adoption of machine learning algorithms for environmental and remote sensing studies is suggested – both machine learning algorithms used in this study indicated high power performance and are robust enough to handle data complexities well. The machine learning models used here

are easily modifiable to fit specificities of any urban region and should therefore be further explored.

- The findings in this study can be used as a benchmark study for further investigation into the spatial distribution and extent of *Fusarium Dieback* infestation in urban street trees, and can be used to guide the development of statistical models that are tailored to suit heterogonous and complex urban environments where greater knowledge gaps exist.
- The shortcomings of this study prove that there is need in the remote sensing industry for better equipped methods of validation, data collection, and methodological approaches to understanding pest-induced infestations in urban forests.
- Several limitations were identified in this study, and are proposed as reasons for the poor performance of the WV-2 image in distinguishing infested trees from healthy ones. These limitations must be taken into consideration when evaluating the feasibility of this study and the proposed solutions must be applied to determine if classification accuracies can be improved for similar pest-related infestation studies.
- Overall, both models were not able to correctly or accurately map infested London Plane trees within the study area.

CHAPTER 6:

Conclusion

This study has shown that the WorldView-2 multispectral data has the potential to detect the *Fusarium Dieback infestation*, if/when combined with scientifically sound approaches of validation, data collection, and methodological approaches. Furthermore, it proves that remote sensing methodologies provide an opportunity to detect and monitor the occurrence of infestations and invasive pest species (ISPs) such as the Polyphagous Shot Hole Borer (PSHB) and should therefore be explored furthermore, particularly in overcoming the drawbacks identified in this study that could likely improve detection accuracies. The study needs to be extended to cover the entire City of Johannesburg region in order to fully synthesize the extent of the *Fusarium Dieback* tree infestation. Multispectral data can be effective and appropriate for long-term, large-scale, real-time assessments of the spread of *Fusarium Dieback* infestation.

The overall aim of the study to determine how accurately WorldView-2 satellite imagery can be used to detect the *Fusarium Dieback infestation* in the London Plane (*Platanus x acerifolia*) tree species was achieved. The findings showed that the overall process failed to accurate detect occurrences of *Fusarium Dieback*, despite mapping the other LULC classes accurately. Several reasons for the low accuracy was provided in the study, which consequently indicated that limitations in reference data collection, analysis, and processing played a significant role. All of the objectives of the study were achieved. Both machine learning algorithms that were used in the study performed equally well with the WorldView-2 imagery. The results per objective could be improved in future studies if the suggested recommendations are implemented, particularly in addressing the several shortfalls identified throughout this study.

The approaches suggested in this paper could be used to map and monitor the spread of *Fusarium Dieback* at larger extents, as well as to aid the development of predictive models based on existing distribution patterns. This will assist in the effort to curb the spread of the disease and provide vital support for management policies and strategies. Knowing where the PSHB invades densely and understanding how its distribution patterns change across various tree species and different climatic regions will enable managers and key stakeholders to make informed decisions about control mechanisms in greater urban landscapes.

Tools such as remote sensing, GIS, machine learning, and other technological advances in the field have provided inexpensive ways for stakeholders to keep track of, and provide updated information on, the severity of spread. Johannesburg, one of the hardest hit urban areas (Paap et al., 2020), should be at the forefront of developing solutions that are innovative and long-term. While location-based solutions are not the key to killing the PSHB, or ridding cities of its harmful *Fusarium Dieback infestation*, these solutions can be the driving force behind managing how the spread of infestation is contained. Knowing where infestations occur most frequently, the type of tree species most infested, and the climates in which the PSHB beetle best thrive are all fundamental aspects of solving one of the greatest pest-invasion crises South Africa has ever faced. This paper, thus, recommends the use of remote sensing tools, such as WorldView-2, to determine and map infested tree species across the City of Johannesburg and other complex urban environments.

As a further research exploration on the *Fusarium Dieback* infestation, studies could investigate canopy structural analyses of infested tree species since one of the main problems in this study was spectral confusion through canopy overlap. Additionally, future studies could focus on degrees of severity, which this study failed to do. In that way, it could be determined if scaling the levels of infestation, without focusing on other LULC classes, would improve classification accuracies and detect *Fusarium Dieback infestation* with greater success.

CHAPTER 7:

References

Abdullah, H., Skidmore, A.K., Darvishzadeh, R., Heurich, M. (2019). Sentinel-2 accurately maps greenattack stage of European spruce bark beetle (Ips typographus, L.) compared with Landsat-8. *Remote Sens Ecol Conserv*, 5, 87–106. https://doi.org/10.1002/rse2.93.

Abutaleb, K., Newete, S. W., Mangwanya, S., Adam, E., Byrne, M. J. (2020). Mapping eucalypts trees using high resolution multispectral images: A study comparing WorldView 2 vs. SPOT 7. *The Egyptian Journal of Remote Sensing and Space Science*, https://doi.org/10.1016/j.ejrs.2020.09.001.

Adam, E., Mutanga, O. Ismail, R. (2013). Determining the susceptibility of Eucalyptus nitens forests to Coryphodema tristis (cossid moth) occurrence in Mpumalanga, South Africa. *International Journal of Geographical Information Science*, 27 (10), 1924 – 1938.

Adam, E., Mureriwa, N., and Newete, E. (2017). Mapping Prosopis glandulosa (mesquite) in the semi-arid environment of South Africa using high-resolution WorldView-2 imagery and machine learning classifiers. *Journal of Arid Environments*, 145, 43 – 51.

Alonzo, M., Bookhage, B., and Roberts, D. A. (2014). Urban tree species mapping using hyperspectral and lidar data fusion. *Remote Sensing of Environment*, 148, 70 – 83.

Anderson, K., & Gaston, K. J. (2013). Lightweight unmanned aerial vehicles will revolutionize spatial ecology. *Frontiers in Ecology and the Environment*, 11 (3), 138–146.

Boissard P, Martin V, Moisan S. (2008). A Cognitive Vision Approach to Early Pest Detection in Greenhouse Crops. *Computers and Electronics in Agriculture*, 62 (2), pp.81-93.

Boland, J. M. (2016). The impact of an invasive ambrosia beetle on the riparian habitats of the Tijuana River Valley, California. *PeerJ* 4:e2141; DOI 10.7717/peerj.2141.

Boreham, G. R. (2006). A survey of cossid moth attack in Eucalyptus nitens on the Mpumalanga Highveld of South Africa. *Southern African Forestry Journal*, 206, (1), 23 – 26.

Breiman, L. (2001). Random forest. *Machine learning*, 45, 5–32.

Byers, J. A., Maoz, Y., Wakarchuk, D., Fefer, D., and Levi-Zada, A. (2018). Inhibitory Effects of Semiochemicals on the Attraction of an Ambrosia Beetle Euwallacea nr. Fornicatus to Quercivorol in *Journal of Chemical Ecology*, 44, 565 – 575.

Campbell, C., Cristianini, N., and Smola, A. (2000), “Instance selection using support vector machines,” submitted to *Machine Learning*.

Carlotto, M. J. (2009). Effect of errors in ground truth on classification accuracy. *International Journal of Remote Sensing*.

Chance, M. C., Coops, N. C., Plowright, A. A., Tooke T. R., Christen, A., Aven, N. (2016). Invasive shrub mapping in an urban environment from hyperspectral and LiDAR-derived attributes. *Frontiers in plant science*, 7, 1528 – 1535.

Dale, A. G., and Frank, S. D. (2014). Urban warming trumps natural enemy regulation of herbivorous pests in *Ecological Applications*, 24 (7), 1596 – 1607.

DigitalGlobe. (2010). The Benefits of the Eight Spectral Bands of WorldView-2.

Dimson, M. (2017). Utility of temporally-biased invasive species distribution models in the detection of Euwallacea sp. nr. fornicatus in California. Los Angeles: *University of California Press*.

Dye, M., Mutanga, O., Ismail, R. (2008). Detecting the severity of Woodwasp, Sirex noctilio, infestation in a pine plantation in KwaZulu-Natal, South Africa, using texture measures calculated from high spatial resolution imagery. *African Entomology*, 16 (2): 00–00 (2008). https://doi.org/10.4001/1021-3589-16.2.263.

Eskalen, A., Stouthamer, R., Lynch, S. C., Twizeyimana, M., Gonzalez, A., and Thibault, T. (2013). Host range of *Fusarium Dieback* and its ambrosia beetle (Coleoptera: Scolytinae) vector in southern California. *Plant Disease*, 97, 938 – 951.

Faithpraise, F., Birch, P., Young, R., Obu, J., Bassey, F., and Chatwin, C. (2013). Automatic Plant Pest Detection and Recognition Using K-Means Clustering Algorithm and Correspondence Filters in *International Journal of Advanced Biotechnology and Research*, 4 (2), 189 – 199.

Fassnacht, F.E., Latifi, H., Ghosh, A., Joshi, P.K., Koch, B. (2014). Assessing the potential of hyperspectral imagery to map bark beetle-induced tree mortality. *Remote Sens Environ*, 140, 533–548. https://doi.org/10.1016/j.rse.2013.09.014.

Freeman, S., Sharon, M., Maymon, M., Mendel, Z., Protasov, A., Aoki, T., Eskalen, A., O'Donnell, K. (2017). Fusarium Euwallaceae sp. nov.—a symbiotic fungus of Euwallacea sp., an invasive ambrosia beetle in Israel and California. *Mycologia*, 105:6, 1595-1606, DOI: 10.3852/13-066.

Forestry and Agricultural Biotechnology Institute. (2019). *The Polyphagous Shot Hole Borer (PSHB) And Its Fungus In South Africa*. Available at: https://www.FABInet.up.ac.za/index.php/pshb. Accessed on 5 April 2019.

Foxcroft, L.C., Van Wilgen, N.J., Baard, J.A., and Cole, N.S. (2017). Biological invasions in South African National Parks. *Bothalia*, 47 (2), a2158.

Fryer, H. (2019). An aggregation of nine datasets from PSHB specialists to represent the susceptibility of South African tree species to PSHB infestation. Available at: https://polyphagous-shot-hole-borer.co.za/pshb/. Accessed 5 April 2019.

Gaertner, M., Novoa, A., Fried, J., and Richardson, D. M. (2017). Managing invasive species in cities: A decision support framework applied to Cape Town. *Biol Invasions*, 19, 3707 – 3723.

Gairola, S., Proches, S., Michael Gebreslasie, S., and Rocchini, D. (2016). Remote sensing object oriented approaches coupled with ecological informatics to map invasive plant species. *South African Journal of Geomatics*, 5 (3), 285 – 300.

Gidudu, A., Hulley, G., and Marwala, T. (2008). Classification of Images Using Support Vector Machines. Department of Electrical and Information Engineering, *University of the Witwatersrand*, Johannesburg.

Gomes, M.F., Maillard, P. (2013). Identification of urban tree crown in a tropical environment using WorldView-2 data: problems and perspectives. *International Society for Optical Engineering*, 8893.

Gomez, D. F., Skelton, J., Steininger, M. S., Stouthamer, R., Rugman-Jones, P., Sittichaya, W., Rbaglia, R. J., and Hulcr, J. (2018). Species Delineation within the Euwallacea fornicatus (Coleoptera: Curculionidae) Complex Revealed by Morphometric and Phylogenetic Analyses. *Insect Systematics and Diversity*, *2 (6): 2*; 1 – 11.

Hartling, S., Sagan, V., Sidike, P., Maimaitijiang, M., and Carron, J. (2019). Urban Tree Species Classification Using a WorldView-2/3 and LiDAR Data Fusion Approach and Deep Learning. *Sensors*, 19, 1- 23.

Immitzer, M., Atzberger, C, and Koukal, T. (2012). Tree species classification with random forest using very high spatial resolution 8-band WorldView-2 satellite data. *Remote Sens*., 4 (9), pp. 2661 – 2693.

Immitzer, M., Atzberger, C. (2014). Early Detection of Bark Beetle Infestation in Norway spruce (Picea

Abies, L.) Using WorldView-2 Data. *Photogramm Fernerkun*, 351 – 367. https://doi.org/10.1127/1432-8364/2014/0229.

Jombo, S., Adam, E., Byrne, J., and Newete, S. W., (2020). Evaluating the capability of WorldView-2 imagery for mapping alien tree species in a heterogeneous urban environment. *Cogent Social Sciences*, 6, 1 – 19.

Li, D., Ke, Y., Gong, H., & Li, X. (2015). Object-based urban tree species classification using bi-temporal WorldView-2 and WorldView-3 images. *Remote Sensing*, 7 (12), 16917 – 16937.

Liu, C. R., Berry, P. M., Dawson, T. P., and Pearson, R. G. (2005). Selecting thresholds of occurrence in the prediction of species distributions. *Ecography*, 28, 3, 85 – 393.

Lofgren, O. (2013). Using WorldView-2 satellite imagery to detect indicators of high species diversity in grasslands. *International journal of applied Earth Observation and Geoinformation*, 18, 22 – 30.

Lynch, S. C., Stouthamer, R., Carrillo, J. D., and Eskalen, A. (2018). Severity of Fusarium Dieback – Shot Hole Borers Analyzed in *The Grove*, pp46 – 50.

Matthews, T., Lo, A. Y., Byrne, J. A. (2015). Reconceptualizing green infrastructure for climate change adaptation: Barriers and drivers for uptake by spatial planners. *Landscape and Urban Planning*, 138, 155 – 163.

Marx, A. (2010). Erkennung von Borkenkaferbefall in Fichtenreinbestanden mit multi-temporalen RapidEye-Satellitenbildern und Datamining-Techniken. *Photogramm Fernerkun*, 243–252. https://doi.org/10.1127/1432-8364/2010/0052.

Mendel, Z., Protasov, A., Sharon, M., Zveibil, A., Yehuda, S. B., O'Donnell, K., Rabaglia, R., Wysoki, M., and Freeman, S. (2012). An Asian ambrosia beetle Euwallacea nr. Fornicatus and its novel symbiotic fungus Fusarium sp. pose a serious threat to the Israeli avocado industry in *Phytoparasitica* 40 (3), 235 – 238.

Monteiro, A. T., Goncalves, J., Fernandes, R., Alves, S., Marcos, B., Lucas, R., Teodoro, A. C., & Honrado, J. (2017). Estimating Invasion Success by Non-Native Trees in a National Park Combining WorldView-2 Very High Resolution Satellite Data and Species Distribution Models. *Diversity*, 9 (6), 1 – 19.

Morales-Barquero, L., Lyons, M. B., Phinn, S. R., and Roelfsema, C. M. (2019). Trends in Remote Sensing Accuracy Assessment Approaches in the Context of Natural Resources in *Remote Sensing*, 11, 2305.

Mountrakis, G., Im, J., and Ogole, C. (2011). Support vector machines in remote sensing: A review. *ISPRS Journal of Photogrammetry and Remote Sensing*, *66*, 247 –2 59.

Mutanga, O., Elhadi, A., and Cho, M. A. (2012). High Density Biomass Estimation for Wetland Vegetation Using WorldView-2 Imagery and Random Forest Regression Algorithm in *International journal of applied Earth Observation and Geoinformation*, 18, 399 – 406.

Myeong, S., Nowak, D. J., & Duggin, M. J. (2006). A temporal analysis of urban forest carbon storage using remote sensing. *Remote Sensing of Environment*, 101(2), 277–282.

Naicker, K., Cukrowska, E., & McCarthy, T. S. (2003). Acid mine drainage arising from gold mining activity in Johannesburg, South Africa and environs. *Environmental Pollution*, 122(1), 29 – 40.

Nasi, R., Honkavaara, E., Lyytikainen-Saarenmaa, P., Blomqvist, M., Litkey, P., Hakala, T., Viljanen, N., Kantola, T., Tanhuanpaa, T., Holopainen, M. (2014). Using UAV-Based Photogrammetry and Hyperspectral Imaging for Mapping Bark Beetle Damage at Tree-Level. *Remote Sens*, 7, 15467–15493. https://doi.org/10.3390/rs71115467.

Odindi, J.O., Adam, E., Ngubane, Z., Mutanga, O. and Slotow, R. (2014). Comparison between WorldView-2 and SPOT-5 images in mapping the bracken fern using the random forest algorithm. *Journal of Applied Remote Sensing*, *8*(1), p.083527.

O'Donnell, K., Sink, S., Libeskind Hadas, R., Hucr, J., Kasson, M. T., Ploetz, R. C., Konkol, J. L., Ploetz, J. N., Carillo, D., Campbell, A., Duncan, R. E., Liyanage, P. N. H., Eskalen, A., Na, F., Geiser, D. M., Bateman, C., Freeman, S., Mendel, Z., Sharon, M., Aoki, T., Cossé, A. A., and Rooney, A. P. (2015).

Discordant phylogenies suggest repeated host shifts in the *Fusarium-Euwallacea* ambrosia beetle mutualism. *Fungal Genet Biol*, *82*, 277 – 290.

Paap, T., de Beer, Z. W., Migliorini, D., Nel, W. J., and Wingfield, M. J. (2018). The polyphagous shot hole borer (PSHB) and its fungal symbiont Fusarium euwallaceae: a new invasion in South Africa. *Australasian Plant Pathology*, 47 (2), 231 – 237.

Paap, T., Wingfield, M. J., De Beer, W., and Roets, F. (2020). Lessons from a major pest invasion: The polyphagous shot hole borer in South Africa in South African Journal of Science, 116 (11/12), Art. #8757, 4 pages. https://doi.org/10.17159/sajs.2020/8757.

Pal, M (2005). Random forest classifier for remote sensing classification, *International Journal of Remote Sensing*, 26, 217 – 222.

Radoux, J., Bogaert, P., Fasbender, D., Defourny, P. (2010): Thematic accuracy assessment of geographic object-based image classification. *International Journal of Geographical Information Science*, 1 – 17.

Raffa, K. F., Gregoire, J. C., and Lindgren, B. S. (2015). Natural History and Ecology of Bark Beetles in *Chemical Ecology*, 37, 820 – 831.

Rodriguez-Galiano, V.F., B. Ghimire, J. Rogan, M. Chica-Olmo & J.P. Rigol-Sanchez. (2012). An assessment of the effectiveness of a random forest classifier for land-cover classification. *Journal of Photogrammetry and Remote Sensing*, 67, 93 – 104.

Schäfer, E., J. Heiskanen, V. Heikinheimo & P. Pellikka (2016). Mapping tree species diversity of a tropical montane forest by unsupervised clustering of airborne imaging spectroscopy data. *Ecological Indicators*, 64, 49 – 58.

Schäffler, A., and Swilling, M. (2012). Valuing green infrastructure in an urban environment under pressure — The Johannesburg case in *Ecological Economics*, 1 – 12.

Senf, C., Seidl, R., Hostert, P. (2017). Remote sensing of forest insect disturbances: Current state and future directions. *Int J Appl Earth Obs Geoinf*, 60, 49–60. https://doi.org/10.1016/j.jag.2017.04.004.

Shojanoori, R., and Shafri, H. Z. (2016). Review on the use of remote sensing for urban forest monitoring. Arboric Urban For, 42 (6), pp. 400 – 417.

Shi, Y. (2020). Remotely sensing the species of individual trees in *International Journal of Applied Earth Observation and Geoinformation, 73*, 207 – 219.

Statistics SA. (2011). http://www.statssa.gov.za/?page_id=1021&id=city-of-johannesburg-municipality Accessed on 17 April 2019.

Stohlgren, T. J., Ma, P., Kumar, S., Rocca, M., Morisette, J. T., Jarnevich, C. S., and Benson, N. (2010). Ensemble Habitat Mapping of Invasive Plant Species. *Risk Analysis, Vol. 30, No. 2.* DOI: 10.1111/j.1539-6924.2009.01343.x.

Stouthamer, R., Rugman-Jones, P., Thu, P. Q., Eskalen, A., Thibault, T., Hulcr, J., Wang, L. J., Jordal, B. H., Chen, C. Y., Cooperband, M., Lin, C. S., Kamata, N., Lu, S. S., Masuya, H., Mendel, Z., Rabaglia, R., Sanguansub, S., Shih, H. H., Sittichaya, W., and Zong, S. (2017). Tracing the origin of a cryptic invader: phylogeography of the Euwallacea fornicatus (Coleoptera: Curculionidae: Scolytinae) species complex. *Agric For Entomol*. https://doi.org/10.1111/afe.12215.

Takenaka, Y., Katoh M., Deng, S., and Cheung K. (2017). Detecting Forests Damaged By Pine Wilt Disease At The Individual Tree Level Using Airborne Laser Data And WorldView-2/3 Images Over Two Seasons in *The International Archives of the Photogrammetry, Remote Sensing and Spatial Information Sciences*, 3.

Thabeng, O. L., Merlo, S., and Adam, E. (2019). High-resolution remote sensing and advanced classification techniques for the prospection of archaeological sites' markers: The case of dung deposits in the Shashi-Limpopo Confluence area (southern Africa). *Journal of Archaeological Science, 102,* 48 – 60.

Umeda, C. Y. (2017). Environmental Effects on Polyphagous Shot Hole Borer (Dissertation): *University of California*, Riverside.

Van den Berg, N., Du Toit, M., Morgan, S. W., Fourie, G., and de Beer, Z. W. (2019). First Report of Fusarium euwallaceae on Persea Americana in South Africa. *Plant Disease*.

Vapnik, V. and Chapelle, O. (1999), "Bounds on error expectation for support vector machines," submitted to *Neural Computation*.

Verlic, A., Kokajl, Z., Marsetic, A., Simoncic, P. (2014). Tree Species Classification using WorldView-2 Satellite Images and Laser Scanning Data in a natural Urban Forest. Sumarski List, 138(9-10), 477 – 488.

Viinikka, A. (2016). Mapping Individual Tree Species Using Airborne Imaging Spectroscopy and Laser Scanning Data in Taita Hills, Kenya (Dissertation). *University of Helsinki*, Helsinki.

Wichmann, L., & Ravn, H. P. (2001). The spread of Ips typographus (L.) (Coleoptera, Scolytidae) attacks following heavy windthrow in Denmark, analysed using GIS. *Forest Ecology and Management*, 148 (1–3), 31 – 39.

Xulu, S., Peerbhay, K. Y., and Gebreslasie, M. (2018). Remote sensing of forest health and vitality: a South African perspective. Southern Forests: a Journal of Forest Science, 10, 1 – 12.

Zafari, A., Zurita-Milla, R. and Izquierdo-Verdiguier, E., 2017, October. Integrating support vector machines and random forests to classify crops in time series of WorldView-2 images. *Image and Signal Processing for Remote Sensing XXIII, 10427*. International Society for Optics and Photonics.

Zhang, C., & Qiu, F. (2012). Mapping individual tree species in an urban forest using airborne lidar data and hyperspectral imagery. *Photogrammetric Engineering & Remote Sensing*, *78, 10*, 1079 – 1087.